

The Lateral Instability of Yielded Mild Steel Beams of Rectangular Cross-Section

B. G. Neal

Phil. Trans. R. Soc. Lond. A 1950 **242**, 197-242

doi: 10.1098/rsta.1950.0001

Email alerting service

Receive free email alerts when new articles cite this article - sign up in the box at the top right-hand corner of the article or click [here](#)

THE LATERAL INSTABILITY OF YIELDED MILD STEEL BEAMS OF RECTANGULAR CROSS-SECTION

By B. G. NEAL,* *Engineering Laboratory, University of Cambridge*

(Communicated by Sir Geoffrey Taylor, F.R.S.—Received 20 December 1948—Revised 4 July 1949)

CONTENTS

	PAGE		PAGE
NOTATION		12. Experimental determination of initial torsional rigidity	198
PART I. THE INITIAL SECONDARY FLEXURAL RIGIDITY	199	(a) Beams in pure bending	220
1. Introduction	199	(i) Tests on a bar of rectangular cross-section	220
2. Statement of the problem	199	(ii) Tests on a bar of circular cross-section	222
3. Stress-strain relation	200	(b) Bending combined with shear	223
4. Bending moment-curvature relations in pure bending	202	PART III. THE CONDITIONS CAUSING LATERAL INSTABILITY	226
5. Initial secondary flexural rigidity for a beam of rectangular cross-section	204	13. Introduction	226
(a) Triangular unloading zones	205	14. Pure bending	226
(b) Trapezoidal unloading zones	206	15. Bending combined with shear	229
6. Initial secondary flexural rigidity for a beam of circular cross-section	207	(a) The governing differential equation	229
7. Experiments on beams of rectangular cross-section	209	(b) Solution by finite difference approximations	230
8. Experiments on beams of circular cross-section	215	(c) Beam with central concentrated load	231
PART II. THE INITIAL TORSIONAL RIGIDITY	217	(d) Cantilever	234
9. Introduction	217	16. Experimental work	235
10. The distribution of shear stress	217	17. Discussion	240
11. Combined elastic and plastic deformation	219	REFERENCES	242

The critical load causing secondary failure of a deep beam by lateral buckling may be calculated by standard methods for those cases in which the beam behaves elastically under the applied load. When, however, the load is sufficiently great to cause partial yield of the beam, these methods give an estimate for the critical load which is too high. In the present paper the phenomenon of lateral buckling in deep mild steel beams of rectangular cross-section is studied from both a theoretical and an experimental standpoint. The paper is divided into three parts.

In part I the critical lateral buckling load is shown to depend on the flexural rigidity of the beam about its weaker principal axis while the applied load, causing flexure about its stronger principal axis, is held constant. The dependence of this rigidity on the extent to which the beam has yielded is calculated, and the results are confirmed by tests on beams of rectangular and circular cross-section. It is also shown that the critical load depends on the initial torsional rigidity of the beam, defined as the initial slope of the torque against angle of twist per unit length relation for torsion about the longitudinal axis of the beam while the applied bending load is held constant.

* Fellow of Trinity Hall.

In part II it is first shown that in a beam which has partially yielded the shear force due to the variation of the applied bending moment along the length of the beam is carried entirely in the central elastic core of the beam. Using the theory of combined elastic and plastic deformation, it is then shown that the initial torsional rigidity remains constant at its value for elastic torsion, and experimental evidence in favour of this conclusion is presented.

Using the results of parts I and II, the conditions causing lateral instability in deep mild steel beams of rectangular cross-section are determined in part III. For a beam bent by pure terminal couples these conditions may be deduced directly, but for the cases of beams subjected to central concentrated loads and of cantilevers a step by step solution of the governing differential equation is necessary. Experimental confirmation is given for the case of pure bending.

NOTATION

A, A_E	overall primary flexural rigidity.
B, B_E	initial secondary flexural rigidity.
C	torsional rigidity.
M_1	primary bending moment.
M_2	secondary bending moment.
M_Y	bending moment at which yield first occurs.
M_p	fully plastic moment.
M_{cr}	critical buckling moment.
T	torque.
F	shear force.
E	Young's modulus.
G	modulus of rigidity.
L	total length of beam.
R	radius of circular beam.
P	concentrated load on cantilever.
W_1, W_2	loads in experimental work.
Y_y, Z_z, Y_z	stresses.
b	semi-breadth of rectangular bar.
d	semi-depth of rectangular bar.
f_L	lower yield stress.
μ	ratio of upper to lower yield stress.
l	{ semi-length of beam with central load. total length of cantilever.
s	length measured along axis of beam.
x	s/l .
p	specifies plastic zone in flexure of beam of rectangular section.
q	specifies unloading zone in flexure of beam of rectangular section.
m	slope of linear regression line.
k	$B/B_E = k.p$. for secondary flexure of beam of rectangular cross-section.
n	number of subdivisions of beam in finite difference method.
r	r th point in finite difference method.
α	angles used in considering flexure of a circular bar.
β	

ϕ	angle of twist in torsion.
ψ	critical angle used in flexure of beam of circular cross-section.
γ	$M_{cr} = \frac{\gamma}{L} \sqrt{BC}$.
κ	curvature.
τ	angle of twist per unit length.
$F(x)$ $f_a(x)$	functions defined for finite difference calculations.
ϵ	small rotation of axes.
η	percentage correction to experimental results.
λ	flow parameter in Prandtl-Reuss equations.
δ	finite difference.
δ_2	lateral deflexion measured in torsion test.
Δ	finite difference correction.
Δ_1, Δ_2	dial gauge readings.

PART I. THE INITIAL SECONDARY FLEXURAL RIGIDITY

1. INTRODUCTION

The current methods of design for steel structures are based on the assumption that a structure becomes unsafe when the yield stress is reached in the most highly stressed member. However, in highly redundant structures, as typified by steel building frames, the load causing collapse of the entire structure is usually considerably greater than the load at which yield first occurs. While at present the allowable load on a structure is usually derived by applying a factor of safety to the load causing yield, it would be more logical to base the allowable load on the load causing complete collapse, and considerable economies could be effected by employing design methods based on the calculation of collapse loads. The development of such design methods has involved extensive investigations into the behaviour of beams subjected to loads in the range between the load at which the most highly stressed fibres yield and the load causing collapse, referred to as the yield range (Baker 1949). Hitherto, however, it has been assumed that beams loaded in the yield range will not fail by lateral instability before their full strength is developed in a direct manner under the collapse load. It has been realized, however, that the allowable loads on long deep beams loaded within the yield range may be determined by the necessity for preventing secondary failure by lateral buckling, and the present work is intended to show how the loads causing lateral buckling for such beams may be calculated. The investigation has been confined to the case of beams of rectangular cross-section.

2. STATEMENT OF THE PROBLEM

It is well known that a thin deep beam, loaded in one plane so as to cause flexure about the stronger, or primary principal axis of the cross-section, may fail by buckling laterally out of that plane. In the ideal case of a beam which is initially perfectly straight and free from twist, deflexion only occurs in the plane of the applied loads until the maximum bending

moment occurring in the beam reaches a critical value, denoted by M_{cr} . Lateral deflexion and twist then develop simultaneously, and the critical lateral buckling load may be obtained by calculating the value of the applied load at which it is possible for the beam to remain in neutral equilibrium in its characteristic mode of buckling in which the lateral displacement and twist are infinitesimal.

The occurrence of lateral instability is therefore governed by the flexural rigidity of the beam about its weaker, or secondary principal axis, and the torsional rigidity about its longitudinal axis, while the applied load remains constant. The former rigidity, referred to as the initial secondary flexural rigidity, B , may be defined as the initial slope of the bending moment-curvature relation for flexure about the secondary principal axis while the applied load remains constant, and a similar definition may be given for the initial torsional rigidity, C . If the length of the beam is L , the value of M_{cr} is given approximately by

$$M_{cr} = \frac{\gamma}{L} \sqrt{BC}, \quad (2.1)$$

where γ is a numerical constant depending on the degree of constraint at the ends of the beam and the nature of the applied load (Timoshenko 1936). It should be noted that this expression needs modification when the torsional properties of the beam are appreciably affected by the degree of restraint against warping of the cross-section at the ends of the beam, but it has been shown (Timoshenko 1921) that such effects are negligible for beams of rectangular cross-section.

The problem is therefore to determine the rigidities B and C , which will be expected to depend on the extent to which the beam has yielded. In part I of this paper it is shown that the value of B falls off progressively with increase of load in the yield range, and the reduction of this rigidity has been calculated for the cases of beams of both rectangular and circular cross-section. Experimental confirmation of the results is given, the work on the beams of circular cross-section having been carried out with a view to providing additional evidence in favour of the theory.

In part II it is shown that the value of C is independent of the state of stress in the beam, and in part III these results are used to calculate the critical condition causing lateral buckling for beams of rectangular cross-section under various types of loading.

3. STRESS-STRAIN RELATION

In the present work, discussion is restricted to mild steel which has been annealed prior to testing. For such steel, showing a pronounced yield point, the stress-strain relation is found to take the form indicated in figure 1.

Hooke's law is obeyed along Oa until the upper yield stress μf_L is reached, after which further straining takes place along bc at a smaller constant stress f_L , the lower yield stress, until strain hardening sets in at c . For a given steel the relation for pure compressive stress is identical with that for pure tensile stress up to the point c where strain hardening begins, as was shown by Smith (1909), Morrison (1939) and others.

If the stress is reduced after yield has occurred a curved line such as de is followed, but it was shown by Howard & Smith (1925) that the initial slope of this line is Young's modulus E , as indicated.

A number of investigators have found that if several tensile tests on different mild steel specimens cut from the same stock are performed, the values of the lower yield stress vary very little from test to test, whereas the values of the upper yield stress show variations which are quite considerable. On this basis, the view has often been advanced that the upper yield point of mild steel represents an unstable condition of the material analogous, for example, to the elevation of the boiling-point of liquids in the absence of nuclei around which bubbles can form (Nakanishi 1929). However, as pointed out by Smith (1909), and Morrison (1939), such variations in the observed values of the upper yield stress are caused by accidental small eccentricities of the applied tensile load, which cause a bending action which is superposed on the uniform extension due to the axial load. For instance, an eccentricity of

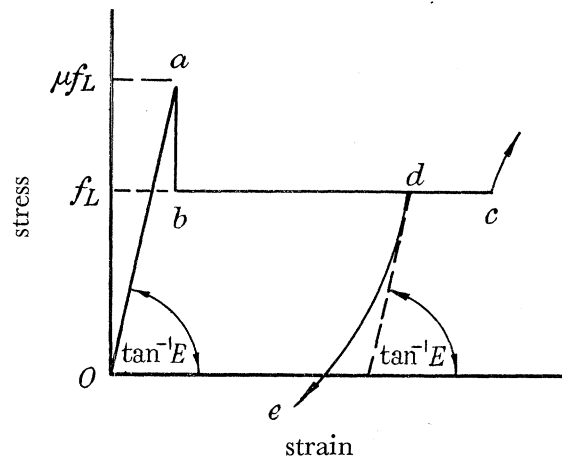


FIGURE 1. Stress-strain relation.

only 0.003 in. causes elastic bending stresses which are 10% of the mean axial stress in a solid circular specimen of 0.25 in. diameter. In such a case yield would be initiated at the point of greatest stress when the mean axial stress was 10% below the upper yield stress. Owing to the drop of stress in the yielded fibres, a correspondingly greater proportion of the load would then be carried by the remainder of the section, so that yield would spread rapidly across the section with a slight increase in load. Thus an accidental eccentricity of load of only 0.003 in. would cause the observed value of the upper yield stress to be nearly 10% less than the true value.

It has also been suggested that in cases of non-uniform stress distribution, as, for example, in the bending of a mild steel beam, yield will begin when the stress at the most highly stressed point reaches the upper yield value, but that once the yielding process has been initiated in this way additional material will yield at the lower yield stress. However, the experiments of Robertson & Cook (1913), and others, have shown that yield always occurs at the upper yield stress, and the experimental work described in the present paper provides further confirmation of this point.

It is well known that the occurrence of yield in mild steel is accompanied by the formation of Lüders lines. It seems probable, as suggested by Muir & Binnie (1926) and others, that the material within the Lüders lines has undergone a considerable amount of slip, and has in fact strained to the point *c* in figure 1. The surrounding material is still entirely elastic, and is sustaining only the lower yield stress. This elastic material is therefore subjected to

a stress considerably below the upper yield stress required to cause elastic breakdown. Further yield as the overall strain is increased must therefore be initiated at points of stress concentration along the boundaries of the Lüders lines, where there will exist 'surfaces of misfit' between adjacent crystals owing to the discontinuity in the amount of slip that has occurred.

This interpretation of the yield phenomenon in mild steel has been borne out by the strain-etch figures obtained by Jevons (1925, 1927) and Nakanishi (1929) for tensile and bend specimens. The work of Jevons, for example, showed very clearly the spread of yield zones from the ends of tensile specimens, where yield was always initiated owing to the stress concentration at the shoulders of the test-pieces.

Acceptance of this physical interpretation of the yield phenomenon implies that the longitudinal strain in a yielded fibre varies discontinuously along the fibre depending on whether the strain is considered at a point in a Lüders line or in elastic material. The relation between longitudinal stress and the average longitudinal strain taken over a considerable length of the fibre will still, however, be as indicated in figure 1. The subsequent work only depends on the nature of this average relation, and therefore holds true irrespective of whether or not this interpretation of the yield phenomenon is accepted.

4. BENDING MOMENT-CURVATURE RELATIONS IN PURE BENDING

When an initially straight beam is bent by pure terminal couples applied about a principal axis of the cross-section, it follows by symmetry that the longitudinal strain varies linearly across the section with distance from some neutral axis. If the bending moment M_1 exceeds the value M_Y at which the upper yield stress is attained in the most highly stressed fibres, the distribution of stress across the section will be as shown in figures 2 and 3 for the cases of rectangular and circular cross-sections, respectively, provided that the outer fibres are not strain hardened. It is assumed, of course, that M_1 has increased steadily from zero.

It may readily be shown (Robertson & Cook 1913) by taking moments about the neutral axis that the relationship between the bending moment M_1 and the curvature κ_1 for the case of a beam of rectangular cross-section is given by

$$\frac{M_1}{M_Y} = 1 + (1 - p^2) \left(\frac{3}{2\mu} - 1 \right), \quad \frac{\kappa_1}{\kappa_Y} = \frac{1}{p}, \quad (4.1)$$

where the bending moment M_Y and curvature κ_Y at which yield first occurs are given by

$$M_Y = \frac{4}{3} \mu f_L b d^2, \quad (4.2)$$

$$\kappa_Y = \frac{\mu f_L}{E d}. \quad (4.3)$$

The relationships between M_1/M_Y and κ_1/κ_Y for values of μ from 1.0 to 1.8 are given in figure 4, from which it will be seen that, if μ exceeds 1.5, equilibrium in the yield range is unstable.

For a beam of circular cross-section the corresponding relations are (Cook 1931)

$$\pi \sin \alpha \frac{M_1}{M_Y} = 2\alpha + \sin 2\alpha + 2 \left(\frac{4}{3\mu} - 1 \right) \sin 2\alpha \cos^2 \alpha, \quad \frac{\kappa_1}{\kappa_Y} = \operatorname{cosec} \alpha, \quad (4.4)$$

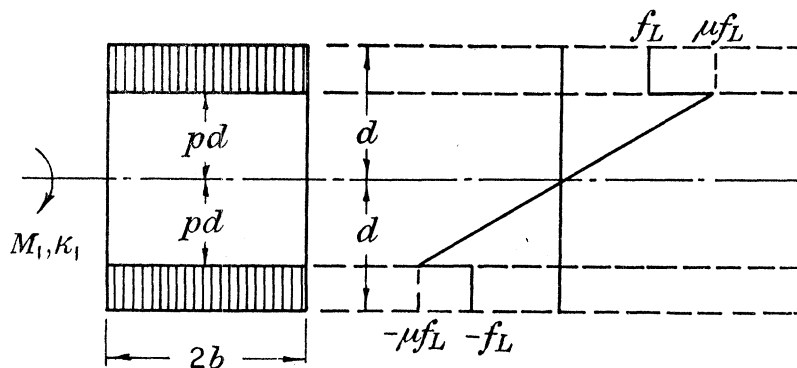


FIGURE 2

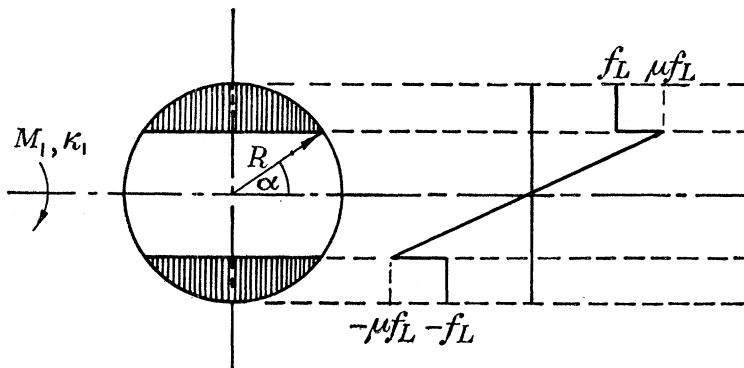


FIGURE 3

FIGURES 2 AND 3. Stress distribution for flexure in the yield range.

|||| zones of yield.

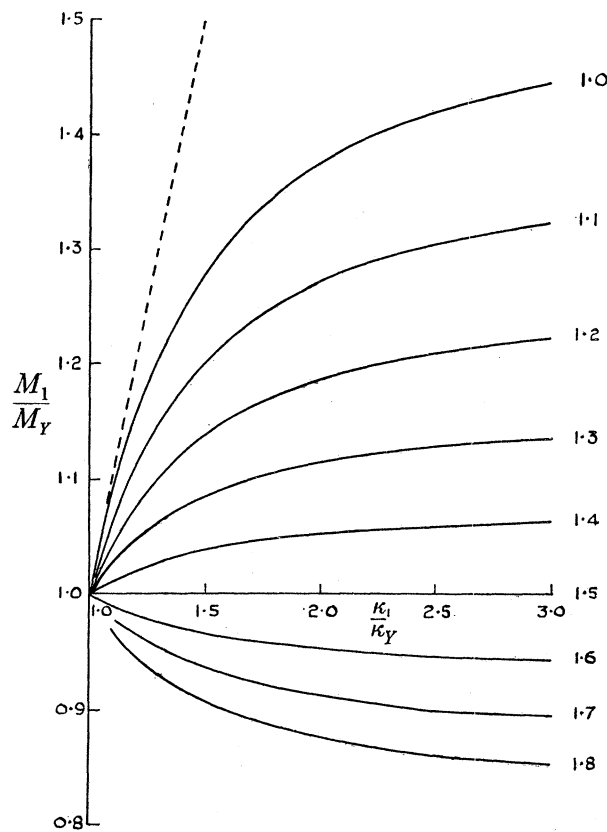


FIGURE 4. Flexure of a beam of rectangular cross-section in the yield range.

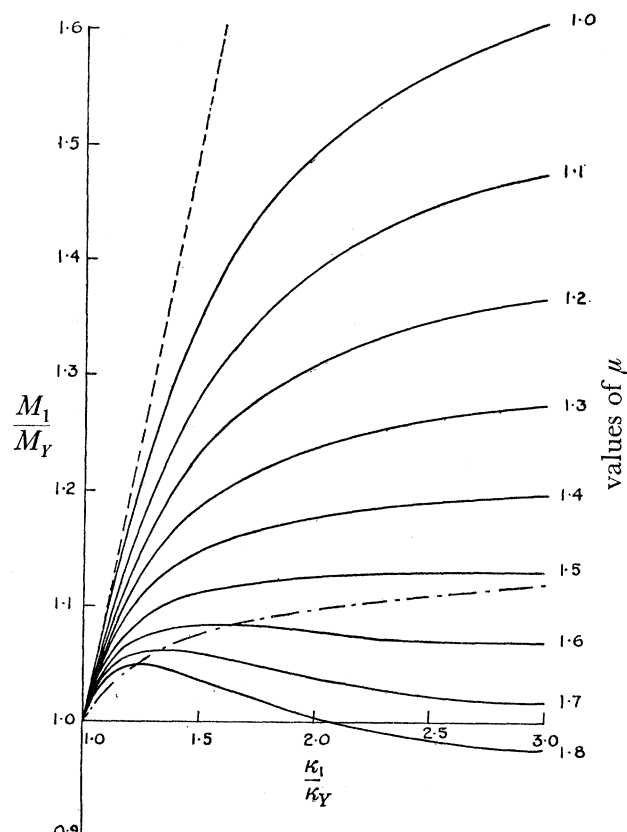


FIGURE 5. Flexure of a beam of circular cross-section in the yield range.

---- Prolongation of elastic line; -.- boundary of stable equilibrium.

where

$$M_Y = \frac{\pi}{4} \mu f_L R^3, \quad (4.5)$$

$$\kappa_Y = \frac{\mu f_L}{ER}. \quad (4.6)$$

The relationships between M_1/M_Y and κ_1/κ_Y for values of μ from 1.0 to 1.8 are given in figure 5, and it will be seen that, if μ exceeds 1.5, equilibrium under M_1 becomes unstable if the curvature exceeds a critical value. It may readily be shown that the value ψ of α at which this occurs is given by

$$2\psi - \sin 2\psi + 6\left(\frac{4}{3\mu} - 1\right) \sin 2\psi \sin^2 \psi = 0, \quad (4.7)$$

and the locus of the maxima of M_1/M_Y is given by

$$3\pi \sin \psi \frac{M_1}{M_Y} = 2\psi (3 - \cot^2 \psi) + \sin 2\psi (3 + \cot^2 \psi). \quad (4.8)$$

5. INITIAL SECONDARY FLEXURAL RIGIDITY FOR A BEAM OF RECTANGULAR CROSS-SECTION

Consider now a beam of rectangular cross-section sustaining a primary bending moment M_1 applied about a principal axis OX , the state of stress at a cross-section being as indicated in figure 2. Suppose that an infinitesimal secondary bending moment dM_2 is applied about the principal axis OY while M_1 remains constant, and let there be increments of curvature $d\kappa_1$ and $d\kappa_2$ about the axes OX and OY , respectively.

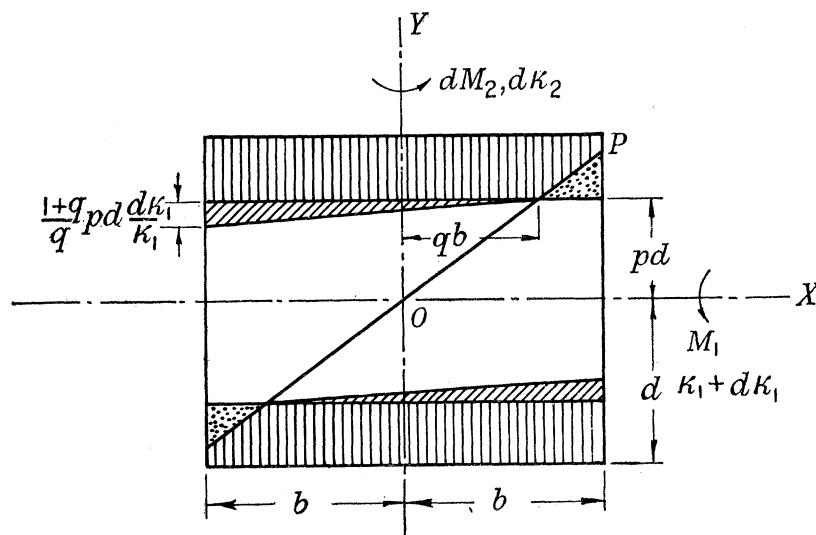

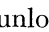



FIGURE 6. Secondary flexure of a beam of rectangular cross-section.  zones of yield due to M_1 alone;  zones of yield due to dM_2 ;  zones of unloading.

The state of stress in the beam will now be as indicated in figure 6. There will exist a straight line OP through the origin along which the longitudinal strain remains unaltered, the slope of this line being

$$\frac{d\kappa_2}{d\kappa_1} = \frac{pd}{qb}. \quad (5.1)$$

It will be shown that q , as defined in figure 6, is always less than 1, so that two zones will form in which the strain is reduced after yield due to M_1 has occurred. These unloading zones may be triangular in shape, as in figure 6, or trapezoidal, depending on whether p is less than or greater than q . Thin triangular zones in which the increment of longitudinal strain due to $d\kappa_1$ and $d\kappa_2$ induces yield will also form, as shown. Each of these zones is a triangle with a base of length $b(1+q)$ and a height of $\left(\frac{1+q}{q}\right)pd\frac{d\kappa_1}{\kappa_1}$.

(a) *Triangular unloading zones*

Consider first the case in which triangular unloading zones form. Small changes in the primary and secondary bending moments may be expected to arise in the following three ways.

- (1) The small changes of strain in the elastic core.
- (2) The finite drop of stress $(\mu-1)f_L$ in the zones of further yield.
- (3) The small reductions of strain in the unloading zones.

Since there is no change in the primary bending moment,

$$\int_0^{pd} 2bEy^2 d\kappa_1 dy - (\mu-1)f_L \frac{1}{2}b(1+q)\left(\frac{1+q}{q}\right)pd\frac{d\kappa_1}{\kappa_1}pd + \int_{pd}^{b\frac{d\kappa_2}{d\kappa_1}} \int_{y\frac{d\kappa_1}{d\kappa_2}}^b E(yd\kappa_1 - xd\kappa_2) y dx dy = 0. \quad (5.2)$$

$$\text{Also, } \frac{1}{2}dM_2 = \int_0^b 2pdEx^2 d\kappa_2 dx - \frac{1}{2}(\mu-1)f_L \left(\frac{1+q}{q}\right)pd\frac{d\kappa_1}{\kappa_1}b(1+q)\left[b - \frac{1}{3}b(1+q)\right] \\ + E \int_{pd}^{b\frac{d\kappa_2}{d\kappa_1}} \int_{y\frac{d\kappa_1}{d\kappa_2}}^b (xd\kappa_2 - yd\kappa_1) x dx dy. \quad (5.3)$$

Relating E to f_L by considering the ratio of stress to strain at the boundaries of the elastic core before secondary flexure commences, we have

$$\mu f_L = Ep d\kappa_1. \quad (5.4)$$

Evaluating the elementary integrals in equation (5.2), and using equation (5.4), it may readily be shown that

$$9q^2\left(\frac{4}{3\mu} - 1\right) + 2q - 1 = 0, \quad (5.5)$$

$$\text{or } q = \frac{\sqrt{(12\mu - 8\mu^2) - \mu}}{12 - 9\mu}, \quad (5.6)$$

the positive value of the radical being selected since p must be greater than zero, and is less than q .

q is thus a function of μ alone when triangular unloading zones form. Values of q for values of μ between 1.0 and 1.5 are shown in figure 7, and it will be seen that q does not exceed 1 unless μ is greater than 1.5. This possibility need not be considered, however, since stable equilibrium under the primary bending moment alone is not then possible.

Remembering that $B = dM_2/d\kappa_2$, and noting that the elastic flexural rigidity for secondary flexure about the axis OY , denoted by B_E , is $\frac{4}{3}Edb^3$, it may be shown from equation (5.3) that

$$\frac{B}{B_E} = \frac{3p(1+q)^2}{16q} \left[\left(\frac{4}{3\mu} - 1\right)q(2-q) + 1 \right]. \quad (5.7)$$

Eliminating μ by using equation (5.5) it is found that

$$\frac{B}{B_E} = \frac{(1+q)^4}{24q^2} p = kp, \quad (5.8)$$

where $k = (1+q)^4/24q^2$ is a function of μ alone, since q is given in terms of μ by equation (5.6).

(b) *Trapezoidal unloading zones*

When p is greater than q the unloading zones are trapezoidal in shape. A similar analysis to the above leads to the result

$$\frac{B}{B_E} = \frac{(1+p)^2}{24p^3} [q^2(p^2 - 2p + 3) + 4qp(p - 2) + 6p^2], \quad (5.9)$$

where q is the solution of

$$q^2 \left[\left(\frac{12}{\mu} - 9 \right) p^4 - 3 \right] + 2q \left[\left(\frac{12}{\mu} - 8 \right) p^4 + 4p \right] + \left(\frac{12}{\mu} - 6 \right) p^4 - 6p^2 = 0. \quad (5.10)$$

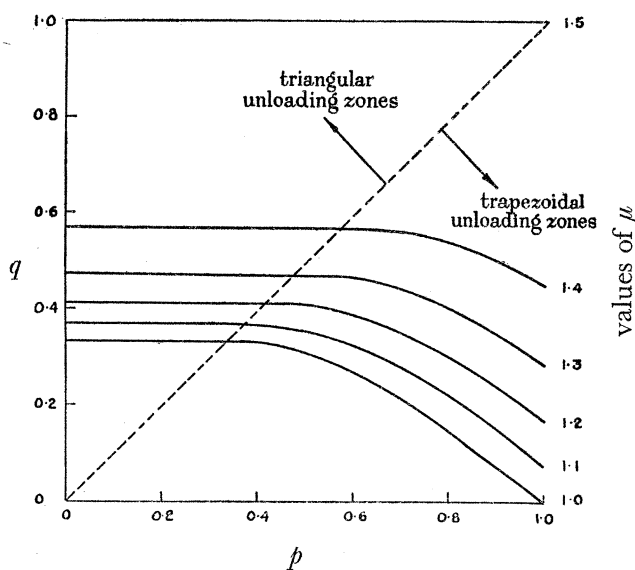


FIGURE 7. Relations between q and p .

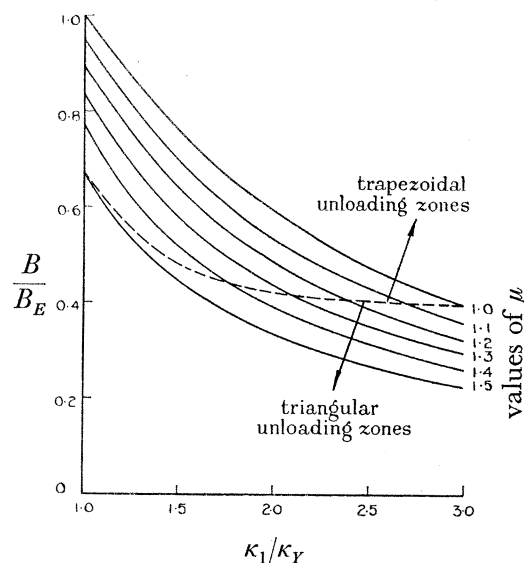


FIGURE 8. The initial secondary flexural rigidity for a beam of rectangular cross-section.

Relations between q and p for values of μ from 1.0 to 1.5 according to equation (5.10) are given in figure 7, and in figure 8 relations between B/B_E and the non-dimensional curvature $\kappa_1/\kappa_Y = 1/p$ according to equations (5.8) and (5.9) are shown.

It is of particular interest to note from figure 8 that a discrete drop in the secondary flexural rigidity takes place for values of μ greater than 1 as soon as yield occurs in the most highly stressed fibres. This discrete drop has an important bearing on the nature of the lateral instability phenomenon in beams of rectangular cross-section, and is a consequence of the finite drop of stress $(\mu - 1)f_L$ occurring in the thin triangular zones of yield which form at the start of secondary flexure.

6. INITIAL SECONDARY FLEXURAL RIGIDITY FOR A BEAM OF CIRCULAR CROSS-SECTION

The state of stress at any section of a beam of circular cross-section sustaining a primary bending moment in the yield range is indicated in figure 3. If an infinitesimal secondary bending moment dM_2 is applied about the secondary principal axis OY while M_1 remains constant, causing increments of curvature $d\kappa_1$ and $d\kappa_2$ to occur about the axes OX and OY respectively, the state of stress will change as shown in figure 9.

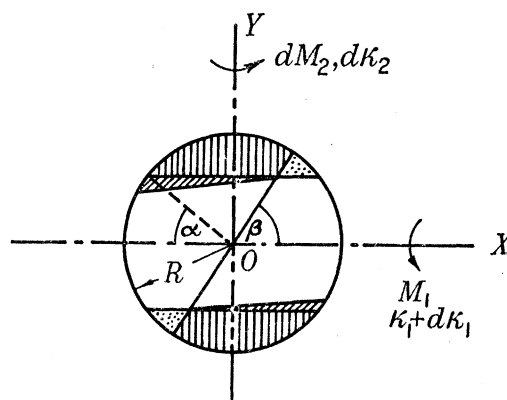


FIGURE 9. Secondary flexure of a beam of circular cross-section. |||| zones of yield due to M_1 alone; // zones of yield due to dM_2 ; . . . zones of unloading.

Unloading zones will form provided that α is less than β , and it is assumed that β is less than $\frac{1}{2}\pi$. An analysis similar to that described in §5 then leads to the result

$$\pi \frac{B}{B_E} = \alpha + \beta + \frac{\sin \alpha}{\sin \beta} \sin(\alpha + \beta) + \left(\frac{4}{3\mu} - 1\right) \sin^4 \alpha (\cot \alpha + \cot \beta)^2 (2 \cot \alpha - \cot \beta), \quad (6.1)$$

where

$$\alpha + \beta - \frac{\cos \alpha}{\cos \beta} \sin(\alpha + \beta) + 3 \tan \beta \left(\frac{4}{3\mu} - 1\right) \sin^4 \alpha (\cot \alpha + \cot \beta)^2 = 0. \quad (6.2)$$

Relations between α and β according to equation (6.2) are shown in figure 10 for values of μ from 1.0 to 1.8, and for values of α between 0 and $\frac{1}{2}\pi$, describing the complete yield range. It will be seen that the values of β exhibited are all less than $\frac{1}{2}\pi$, as assumed. When μ exceeds 1.5, however, α is only less than β for values of α greater than a critical value ψ , dependent on μ . This critical value may be obtained by putting $\alpha = \beta = \psi$ in equation (6.2), which is at once seen to yield equation (4.7), which determines the boundary of stable equilibrium under M_1 alone. It is therefore unnecessary to carry out a further analysis for those cases in which unloading zones fail to form, as the equilibrium under M_1 is then unstable.

Relations between the curvature ratio $d\kappa_1/d\kappa_2 = \cot \beta$ and $\kappa_1/\kappa_Y = \operatorname{cosec} \alpha$ are given in figure 11 for values of μ for 1.0 to 1.8, and in figure 12 the corresponding relations between B/B_E and κ_1/κ_Y are shown.

The equation to the boundary of stable equilibrium in figure 12 may be determined by putting $\alpha = \beta = \psi$ in equation (6.1), and eliminating μ by means of equation (4.7), giving

$$3\pi \frac{B}{B_E} = 2\psi(3 - \cot^2 \psi) + \sin 2\psi(3 + \cot^2 \psi). \quad (6.3)$$

Reference to equation (4.8) then shows that this boundary equation may be put in the very simple form

$$\frac{B}{B_E} = \frac{M_1}{M_Y} \sin \psi. \quad (6.4)$$

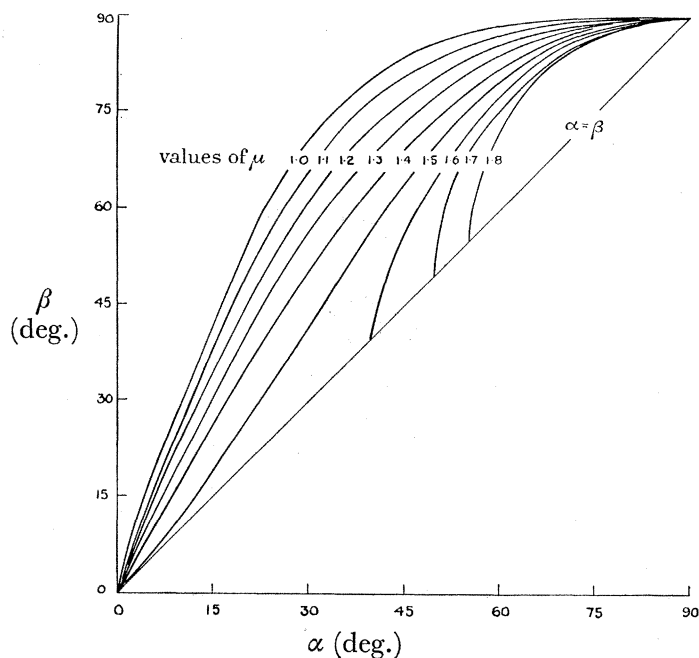


FIGURE 10. Relations between α and β .

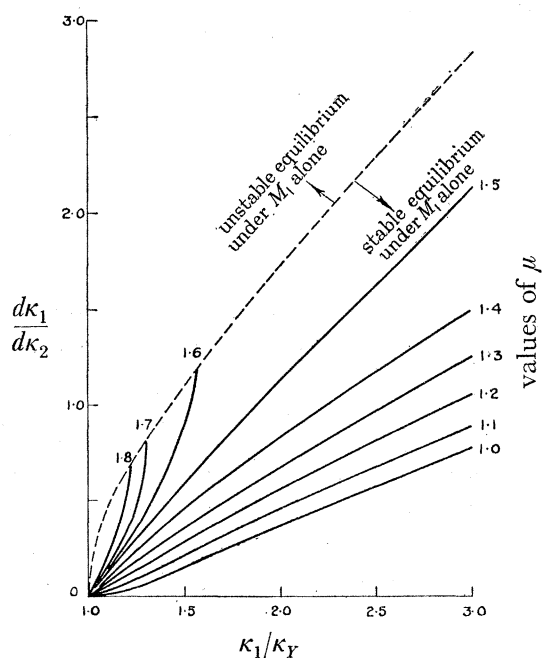


FIGURE 11. Curvature ratio for a beam of circular cross-section.

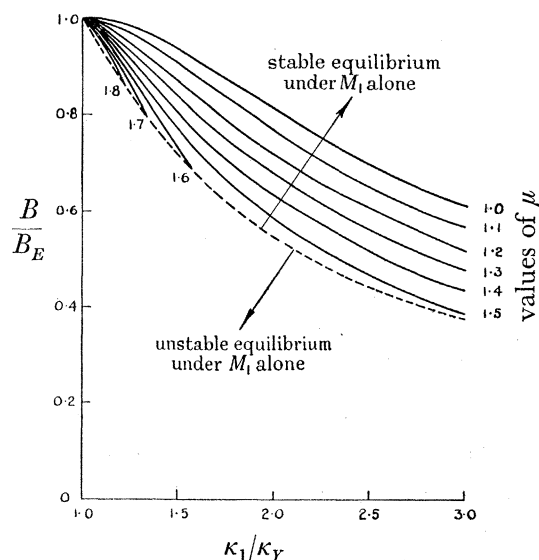


FIGURE 12. Initial secondary flexural rigidity for a beam of circular cross-section.

The significance of this simple expression may be appreciated by considering the special case in which the equilibrium under M_1 is neutral. In this case a small increase in primary curvature, or in other words a small decrease in the depth of the elastic core, leaves the primary bending moment M_1 unchanged.

Consider now the case of neutral equilibrium under a primary bending moment M_1 applied about the axis OX , as shown in figure 13, producing elastic-plastic boundaries AB and CD parallel to OX . If these boundaries are changed to AB' and CD' , parallel to an axis OX' produced from OX by a small anti-clockwise rotation ϵ , then by definition of neutral equilibrium the fresh stress distribution gives rise to a moment M_1 about the axis OX' , the curvature about this axis being say $\kappa_1 + d\kappa_1$. To the first order of small quantities this moment may be resolved into a moment M_1 about OX together with a moment $M_1\epsilon$ about OY .

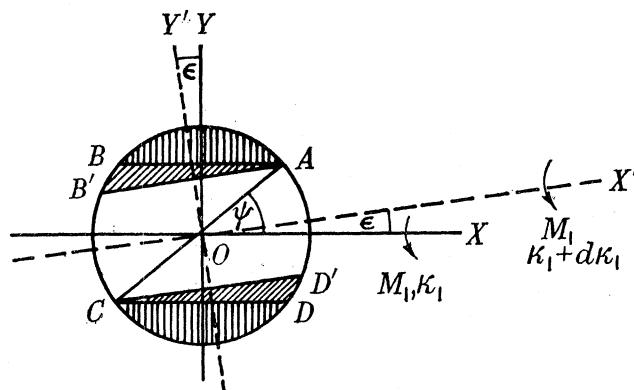


FIGURE 13. Neutral equilibrium.

This may therefore be considered as a case of secondary flexure about OY with the primary bending moment about OX held constant at M_1 . We have

$$dM_2 = M_1\epsilon,$$

$$d\kappa_2 = (\kappa_1 + d\kappa_1)\epsilon = \kappa_1\epsilon,$$

so that

$$\frac{dM_2}{d\kappa_2} = B = \frac{M_1}{\kappa_1} = \frac{M_1 \kappa_Y M_Y}{M_Y \kappa_1 \kappa_Y} = \frac{M_1}{M_Y} \sin \psi B_E,$$

agreeing with equation (6.4).

Thus when the equilibrium under M_1 is neutral the condition that the primary bending moment remains constant to the first order of small quantities is fulfilled when the unloading zones just vanish, so that $\alpha = \beta = \psi$.

7. EXPERIMENTS ON BEAMS OF RECTANGULAR CROSS-SECTION

The test-pieces used in this experimental work were of nominal $\frac{1}{2} \times \frac{1}{4}$ in. rectangular cross-section, faired at their ends by radii into $\frac{3}{4}$ in. diameter ends on which 1 in. of B.S.F. thread was cut. Details of the test pieces are given in figure 14.

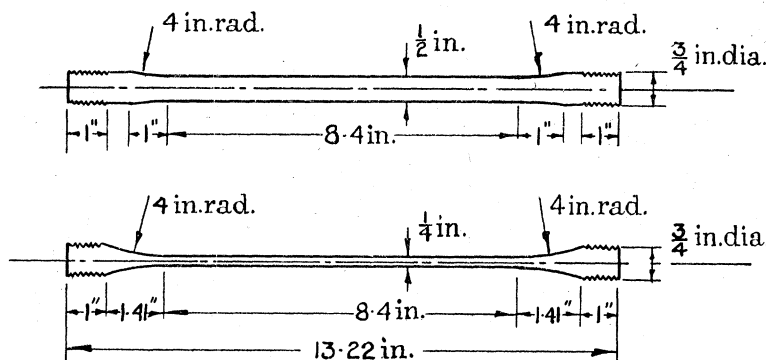


FIGURE 14. Test-pieces of rectangular cross-section.

After machining and final grinding the test-pieces were annealed in sealed steel tubes containing an inert atmosphere of argon. The temperature was maintained at 850°C for 10 min., and the cooling rate was such that the temperature was reduced to 200°C after a further hour.

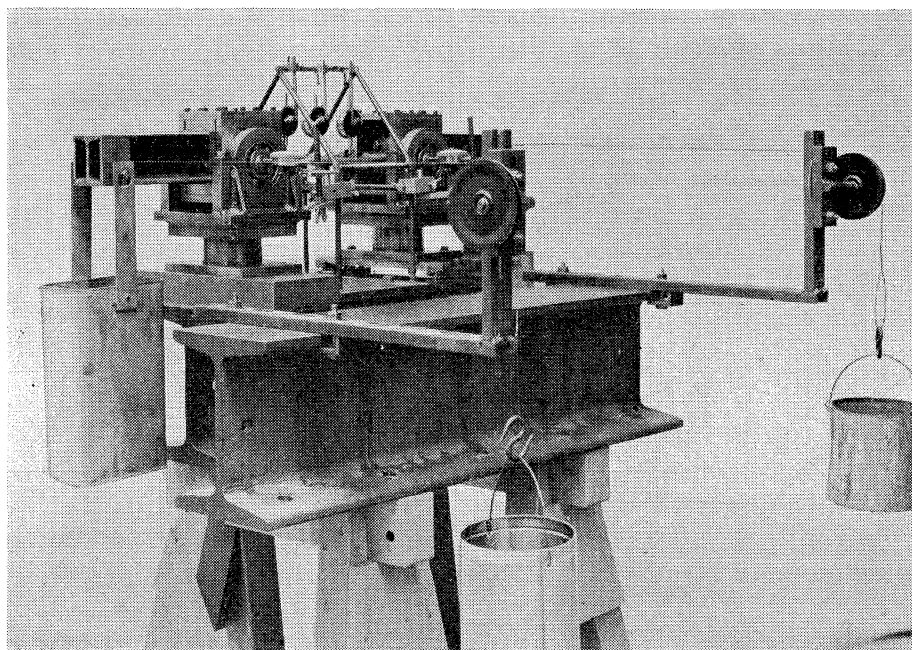


FIGURE 15

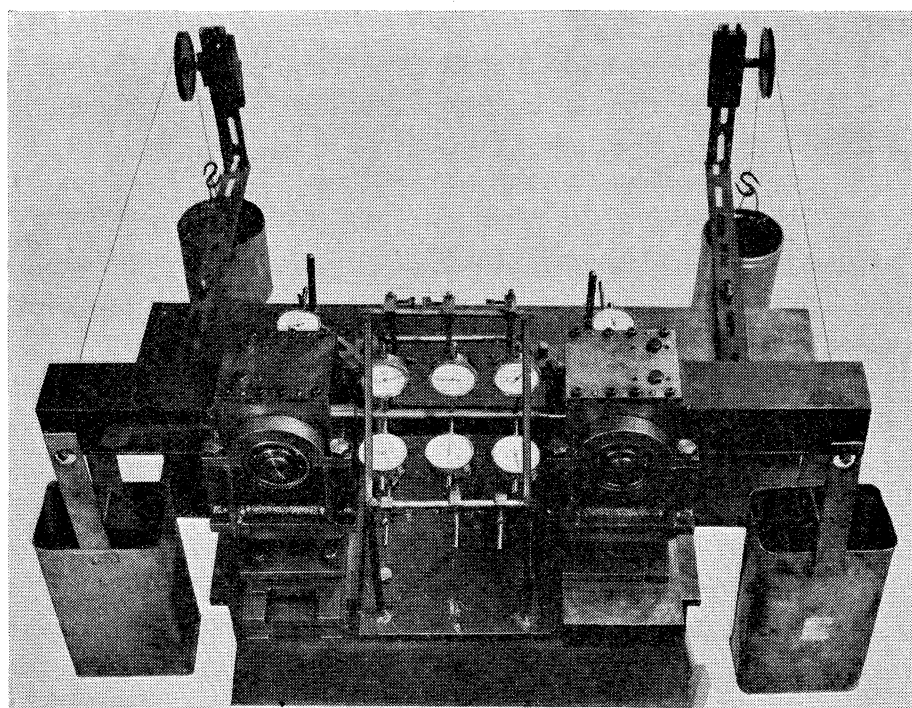


FIGURE 16

YIELDED MILD STEEL BEAMS

211

The composition of the steel is given in table 1.

TABLE 1

element percentage	C	Si	Mn	Ni	Cr	P	S	Al
	0.27	0.26	0.70	nil	0.13	0.05	0.027	0.06

The apparatus used for the tests was as shown in figures 15 and 16. The ends of the test-piece were held in end-fittings, details of which are given in figures 17 and 18. It will be seen from these figures that each end of the test-piece was screwed into a frame which was mounted on a pair of ball journals whose axes were horizontal. These journals were in turn

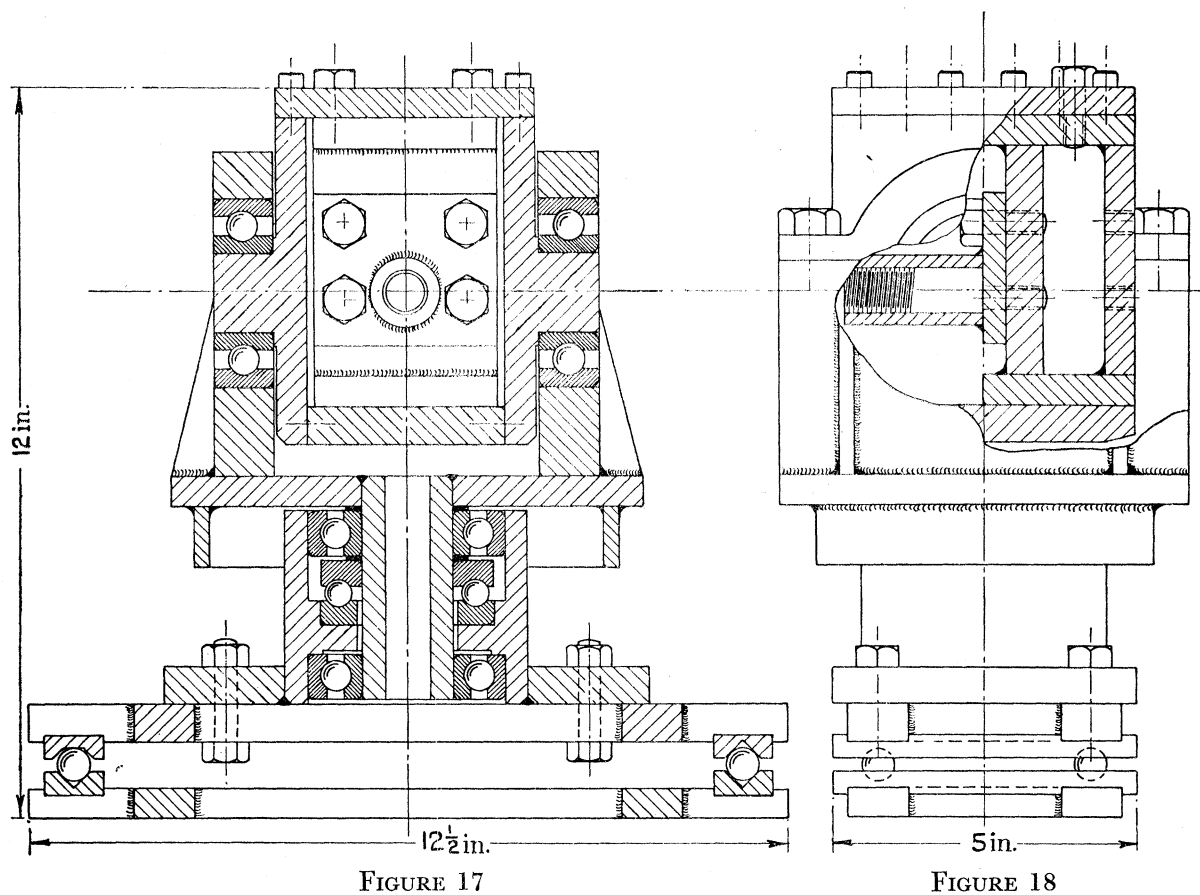


FIGURE 17

FIGURE 18

FIGURES 17 AND 18. End-fittings.

mounted in another frame which was free to rotate about a vertical axis. This freedom was secured by means of a further pair of ball journals together with a thrust bearing to take the vertical load on the end-fitting. The ball journals were provided in order to prevent twist about the longitudinal axis of the specimen. To ensure that no axial force could develop, one of the end-fittings was mounted on two longitudinal rows of balls.

Loading levers were bolted to each end-fitting so that their axes were parallel to the axis of the specimen. The primary bending moment was applied through these loading levers by means of buckets loaded equally with lead shot and supported on horizontal knife-edges, the lever arm being 10 in. The secondary bending moment was also applied through the

loading levers by means of two lengths of piano wire, passing over pulleys mounted on small ball races, and supporting buckets loaded equally with lead shot, the lever arm again being 10 in.

Three standard Mercer dial gauges of the plunger type, capable of reading to the nearest 0·0001 in., were employed for the measurement of deflexions in both the horizontal and vertical planes, being spaced 3 in. apart. Since it was necessary to employ small increments of load, particularly during secondary flexure, the deflexion of a central gauge relative to the two outer gauges was not large enough to be taken as a measure of the curvature. As the deflexion of each gauge was mainly due to the curvature of the central portion of the test-piece of constant cross-section, the sum of the readings of the three dial gauges in one plane was taken as proportional to the curvature, after a correction of about 10 % due to the faired ends of the test-piece and the screwed grips, derived from preliminary calibrations, had been made. A further small correction to the deflexions in the horizontal plane was due to a small lateral deflexion of each end-fitting during secondary flexure, recorded by the two further dial gauges shown in figure 16. As slight variations in the values of the yield stresses and the dimensions of the cross-section along the length of the specimen would cause non-uniform curvature during flexure in the yield range, the method of summing three dial gauge readings has an advantage in indicating closely the mean curvature along the test-piece. If, for instance, the curvature varies linearly along the test-piece the mean curvature is measured exactly in this way.

Despite the use of screwed grips, no trouble was experienced with backlash, presumably because the threads were always sustaining a heavy load arising from the primary bending moment. Friction in the thrust bearings was found to correspond to a coefficient of friction of about 0·007, so that with a primary bucket load of about 60 lb., as used in the tests, the friction torque was about 0·45 lb.in., acting about the secondary axis. Since increments of secondary bending moment of 10 or 20 lb.in. were employed in the tests, this torque was small but not negligible. Its effect was minimized by applying a momentary light pull to the secondary loading wires before the start of secondary flexure, so that the friction torque acted in the same sense throughout the test.

The procedure adopted during each test was to apply successive 50 lb.in. increments of primary bending moment until it became evident that the yield stress had been reached in the outer fibres. Smaller increments of about 10 lb.in. were then applied until secondary flexure began. Successive increments of 10 or 20 lb.in. were then made in the secondary bending moment, while the primary loads were left unaltered.

Four tests, designated R. 1 to 4, were carried out. The relation between the bending moment and curvature during the primary flexure in the yield range for a typical test, R. 4, is shown in figure 19. In this figure the primary bending moment M_1 is shown plotted against Δ_1 , where Δ_1 is the sum of the readings of the three primary dial gauges corrected as already described.

A theoretical curve, calculated in accordance with equation (4·1), is shown in the figure. In fitting this curve, two parameters were available for selection, which may most conveniently be specified as M_y and μ . These parameters were determined with an accuracy of $\pm 0\cdot5\%$ by making the theoretical curve pass through the last observation taken during primary flexure and then adjusting to give the best degree of fit with the other observations.

From the theoretical curve the value of κ_1/κ_Y at the commencement of secondary flexure could readily be calculated. The predicted values of B/B_E and dk_1/dk_2 during secondary flexure could therefore be read off from the curves in figures 7 and 8. These values, together with the corresponding values of the upper and lower yield stresses, are given in table 2 for each test.

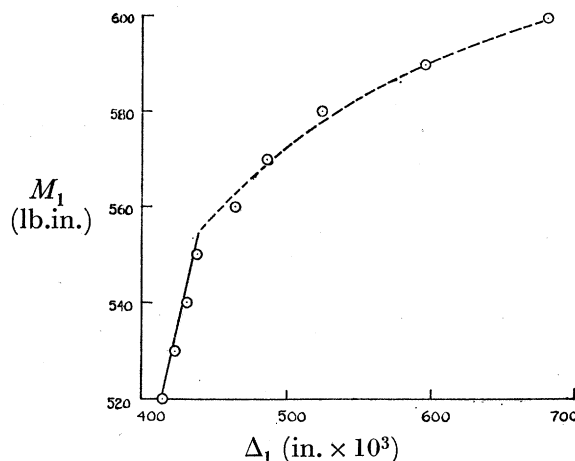


FIGURE 19. Primary flexure, test R. 4.

TABLE 2

test	f_L (tons/sq.in.)	μf_L (tons/sq.in.)	μ	κ_1/κ_Y	B/B_E	dk_1/dk_2
R. 1	18.5	23.1	1.25	1.10	0.81	0.16
R. 2	17.8	23.2	1.30	1.32	0.66	0.28
R. 3	18.0	23.0	1.28	1.38	0.65	0.28
R. 4	17.8	23.5	1.32	1.54	0.56	0.36

The observations taken during secondary flexure with the primary bending moment held constant are given in figures 20 to 23. In these figures the secondary bending moment M_2 is shown plotted against both Δ_1 and Δ_2 , Δ_2 being the sum of the readings of the three secondary dial gauges corrected as previously described.

For elastic secondary flexure the slope of the linear relation between M_2 and Δ_2 could be calculated from a knowledge of the dimensions of the specimen and the proportions of the apparatus. The predicted initial slopes of the relations between M_2 and Δ_1 and Δ_2 during secondary flexure were then calculated from the values of B/B_E and dk_1/dk_2 given in table 2. Straight lines with these predicted slopes, together with the relation between M_2 and Δ_2 for elastic flexure, are given in figures 20 to 23. It will be seen that an excellent degree of agreement exists between the experimental observations and the theoretical predictions.

Test R. 1 is of particular interest in confirming that a discrete drop in the value of the secondary flexural rigidity occurs as the upper yield stress is attained in the outermost fibres. Although the value of κ_1/κ_Y was only 1.10, a predicted drop of 19% in the secondary flexural rigidity was confirmed with considerable precision.

A few attempts were made to carry out further tests at values of κ_1/κ_Y in the neighbourhood of 2. It was found, however, that the primary curvature became markedly non-uniform for such values of the mean curvature, owing to small variations in the yield stresses and dimensions of the specimens.

Application of an increment of load during flexure in the yield range is followed by creep of the deflexion readings. Typical creep curves obtained during test R.2 are shown in figures 24 and 25. During both primary and secondary flexure the deflexions which take

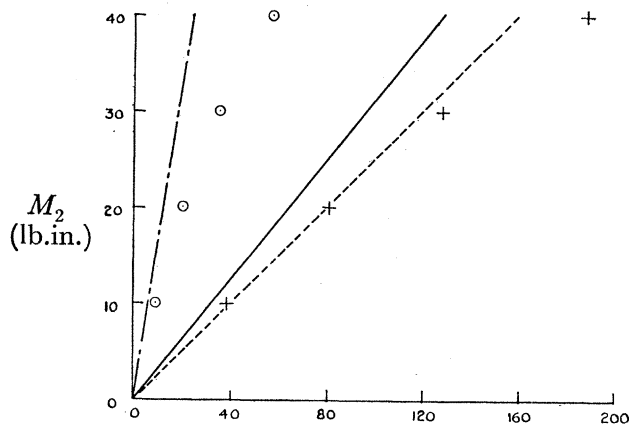


FIGURE 20. Test R. 1.

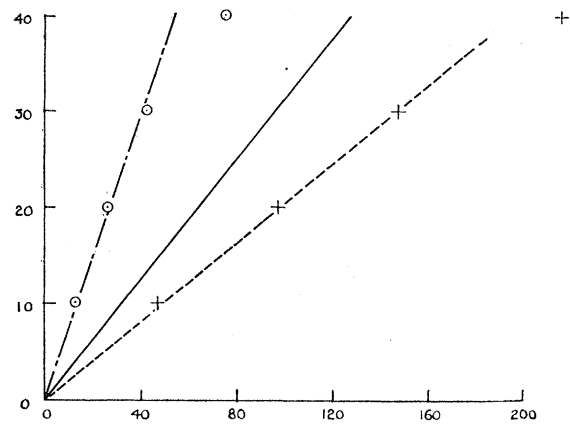


FIGURE 21. Test R. 2.

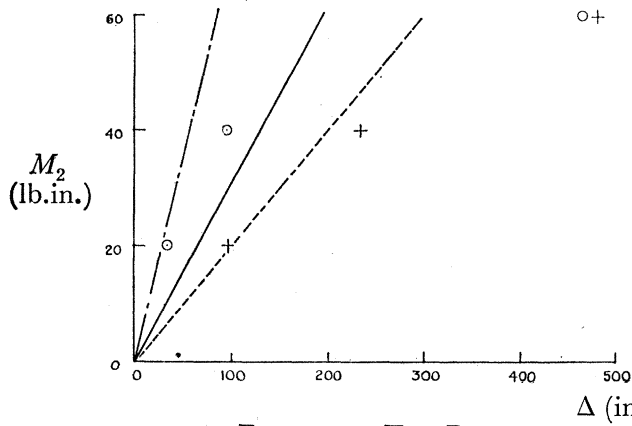


FIGURE 22. Test R. 3.

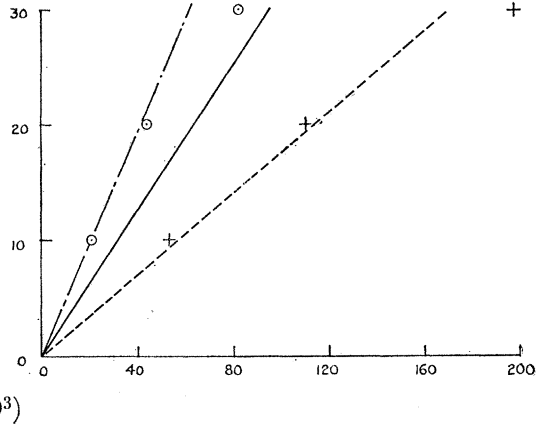
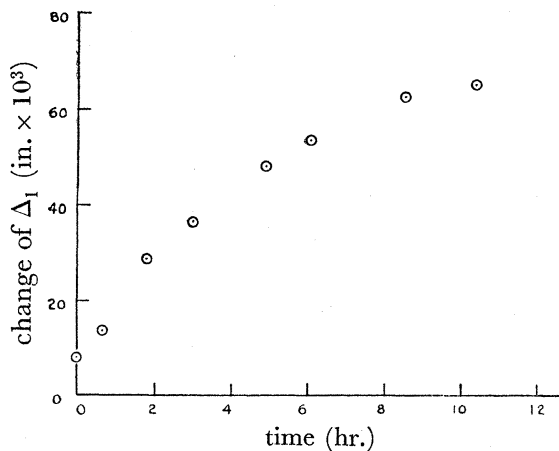
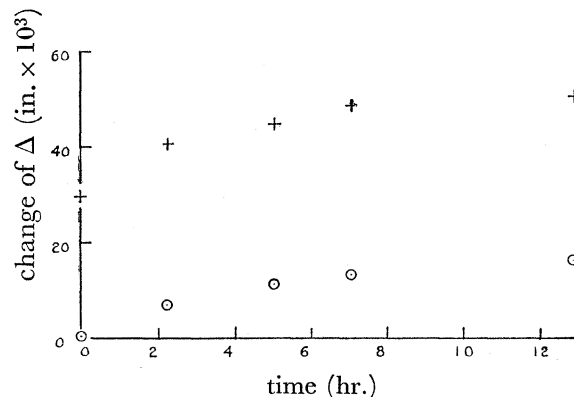


FIGURE 23. Test R. 4.

FIGURES 20 TO 23. Secondary flexure: tests R. 1 to 4. --- theoretical initial slope $dM_2/d\Delta_1$; -.- theoretical initial slope $dM_2/d\Delta_2$; — elastic secondary rigidity; \odot observations of Δ_1 ; + observation of Δ_2 .

FIGURE 24. Test R. 2. M_1 increased from 570 to 580 lb.in.FIGURE 25. Test R. 2. M_2 increased from 20 to 30 lb.in.

\odot observations of Δ_1 ; + observations of Δ_2 .

place instantaneously on the application of a load increment are calculable on the assumption of wholly elastic behaviour. The subsequent plastic flow which then occurs takes several hours for completion.

It will be seen from figures 24 and 25 that the observations taken during the plastic flow lie on curves which are roughly of exponential form. A tentative physical explanation of the nature of the flow process may be given with reference to the formation of Lüders lines in the yielded regions. During flexure in the yield range, Lüders lines will have penetrated from the outer surface of the beam to the boundary between the elastic and yielded material. When the beam is in equilibrium under the applied loads it may be supposed from the discussion of the nature of Lüders lines in § 3 that the tips of the Lüders lines on this boundary will be causing a stress concentration which is just equal to the ratio of the upper to the lower yield stress. On the application of an increment of load this stress concentration will increase by a small amount, causing a tendency for the Lüders lines to penetrate further into the elastic core of the beam until equilibrium is again attained. If all the Lüders lines were of equal size, it might be supposed that there was an equal probability of each one completing its further penetration in any given interval of time, and in this case the relation between the overall change of curvature and time would be of exponential form. In actual fact the creep observations cannot be fitted exactly by curves of exponential form, and the discrepancy may be ascribed to the fact that the Lüders lines vary widely in size.

8. EXPERIMENTS ON BEAMS OF CIRCULAR CROSS-SECTION

The test-pieces used in this experimental work were nominally of $\frac{1}{2}$ in. diameter cross-section, faired at their ends by radii into $\frac{3}{4}$ in. diameter ends on which 1 in. of B.S.F. thread was cut. Detailed dimensions are given in figure 26.

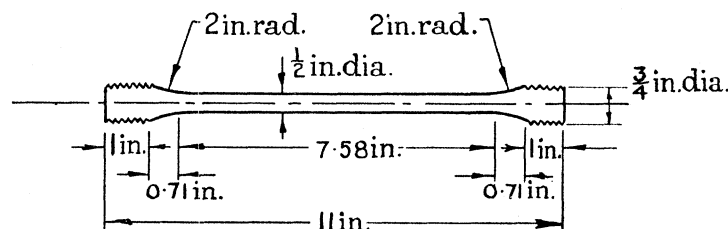


FIGURE 26. Test-pieces of circular cross-section.

The steel was drawn from the same stock as used for the test-pieces of rectangular cross-section, described in § 7, and the test-pieces were subjected to a similar heat treatment after machining and final grinding. The apparatus for the tests was identical with that used for the beams of rectangular cross-section.

Six tests, designated C. 1 to 6, were carried out. The bending moment M_1 during the primary flexure in a typical test, C. 6, is shown plotted against the sum of the three primary dial gauge readings Δ_1 in figure 27. A theoretical curve calculated in accordance with equation (4.4) is also shown.

The value of κ_1/κ_Y at the commencement of secondary flexure then being known, the predicted values of B/B_E and $d\kappa_1/d\kappa_2$ during secondary flexure were read off from the curves of figures 11 and 12. These values, together with the corresponding values of the upper and lower yield stresses, are given in table 3 for each test.

The observations taken during secondary flexure are plotted in figures 28 to 33. In these figures straight lines corresponding to the predicted initial slopes of the relations between M_2 and Δ_1 and Δ_2 are also given, the slopes of these lines being calculated from the values of B/B_E and dk_1/dk_2 given in table 3. It will be seen from these figures that an excellent measure of agreement exists between the experimental observations and the theoretical predictions, although in a few cases the observations of the primary curvature increments are somewhat erratic.

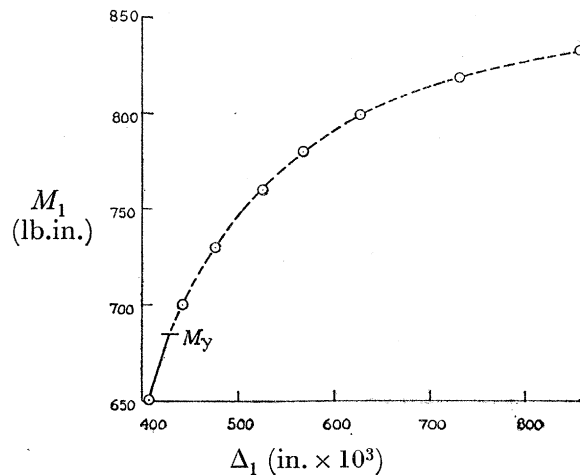


FIGURE 27. Primary flexure, Test C. 6.

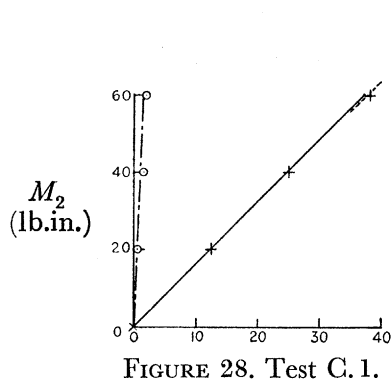


FIGURE 28. Test C. 1.

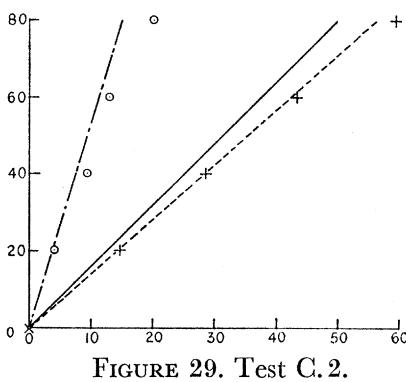


FIGURE 29. Test C. 2.

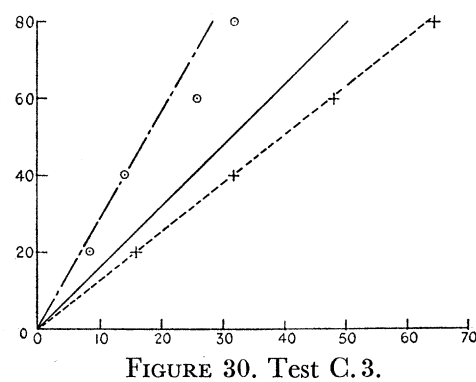


FIGURE 30. Test C. 3.

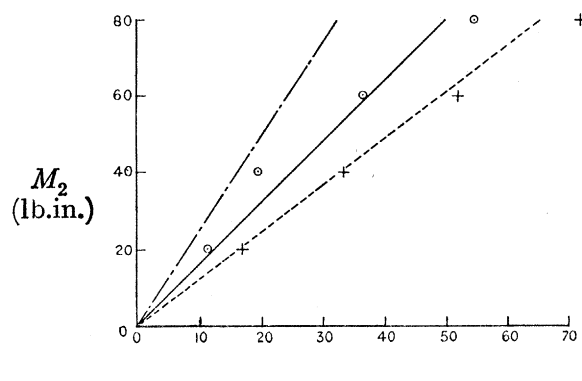


FIGURE 31. Test C. 4.

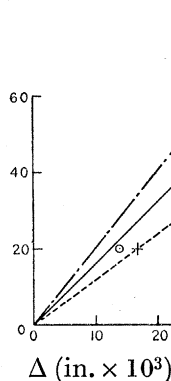


FIGURE 32. Test C. 5.

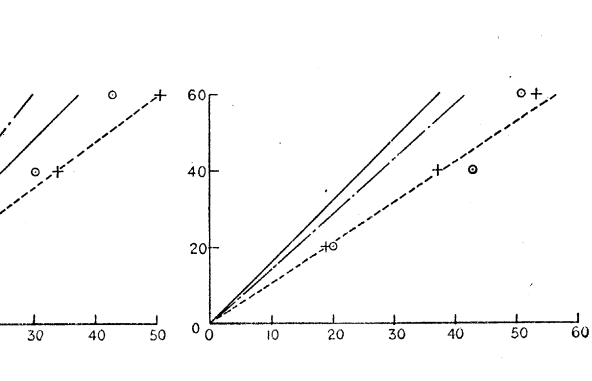


FIGURE 33. Test C. 6.

FIGURES 28 TO 33. Secondary flexure: tests C. 1 to 6. — theoretical initial slope $dM_2/d\Delta_1$; ---- theoretical initial slope $dM_2/d\Delta_2$; — elastic secondary rigidity; ○ observations of Δ_1 ; + observations of Δ_2 .

TABLE 3

test	f_L (tons/sq.in.)	μf_L (tons/sq.in.)	μ	κ_1/κ_Y	B/B_E	$d\kappa_1/d\kappa_2$
C. 1	—	—	1.3*	1.05	0.99	0.04
C. 2	18.6	24.6	1.32	1.35	0.89	0.27
C. 3	18.5	24.6	1.33	1.59	0.80	0.45
C. 4	18.9	24.4	1.29	1.72	0.77	0.50
C. 5	18.6	24.5	1.32	1.76	0.74	0.57
C. 6	18.6	24.8	1.33	2.00	0.66	0.73

* This value of μ was assumed as only one observation was made in the yield range.

The sensitivity of the primary curvature to changes in the value of M_Y , arising from small variations in the dimensions of the cross-section and the values of the yield stresses, was somewhat smaller than in the case of beams of rectangular cross-section. Thus while the highest value of κ_1/κ_Y attained during the series of tests on beams of rectangular cross-section was 1.54 in test R. 4, it was possible in test C. 6 to continue the primary flexure until κ_1/κ_Y was 2.00.

PART II. THE INITIAL TORSIONAL RIGIDITY

9. INTRODUCTION

In part I of this paper it was shown that the prediction of the critical load causing lateral instability in a beam involved a knowledge of the initial torsional rigidity of the beam. This rigidity may be defined as the initial slope of the relation between the torque and angle of twist per unit length for torsion of the beam about its longitudinal axis while the applied bending load is held constant.

In the present paper the value of this rigidity for mild steel beams subjected to bending loads sufficient to cause partial yield is discussed. As a consequence of the theory of combined elastic and plastic deformation, it is shown that the initial torsional rigidity may be expected to remain at its elastic value, irrespective of the extent to which the beam has yielded, provided that there are no shear stresses existing in the yielded regions of the beam. This is clearly true in the case of a beam bent by pure terminal couples, but it is shown in a preliminary analysis that this is also the case when the bending moment varies along the length of the beam, so that a shear force exists. In this case the shear force is carried entirely by a system of shear stresses in the central elastic core of the beam.

10. THE DISTRIBUTION OF SHEAR STRESS

Consider first a beam of rectangular cross-section, and suppose that at any section there exists a bending moment M_1 and a shear force F , as indicated in figure 34, it being assumed that M_1 is sufficiently great to cause partial yield. It will be assumed that the stress system is two-dimensional, so that the only stress components arising are the normal stresses Y_y and Z_z and the shear stress Y_z , adopting the notation of Love (1920).

In the yielded regions some function of the stresses remains constant. Assuming, for example, the von Mises-Hencky criterion for yield, that the strain energy due to change of shape remains constant,

$$Y_y^2 - Y_y Z_z + Z_z^2 + 3Y_z^2 = f_L^2, \quad (10.1)$$

where f_L is the lower yield stress in pure tension or compression.

The two equations of equilibrium are

$$\frac{\partial Y_y}{\partial y} + \frac{\partial Y_z}{\partial z} = 0, \quad (10\cdot2)$$

$$\frac{\partial Y_z}{\partial y} + \frac{\partial Z_z}{\partial z} = 0, \quad (10\cdot3)$$

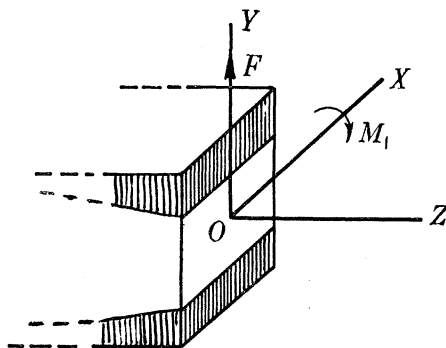


FIGURE 34. Axes and notation. |||| zones of yield.

and the boundary conditions at the outer surface of the beam are $Y_y = Y_z = 0$, $Z_z = f_L$.

By differentiating equation (10·1) it may be shown that

$$\frac{\partial Z_z}{\partial y} \left(2 - \frac{Y_y}{Z_z} \right) - \frac{\partial Y_y}{\partial y} \left(1 - 2 \frac{Y_y}{Z_z} \right) + 6 \frac{Y_z}{Z_z} \frac{\partial Y_z}{\partial y} = 0, \quad (10\cdot4)$$

$$\frac{\partial Z_z}{\partial z} \left(2 - \frac{Y_y}{Z_z} \right) - \frac{\partial Y_y}{\partial z} \left(1 - 2 \frac{Y_y}{Z_z} \right) + 6 \frac{Y_z}{Z_z} \frac{\partial Y_z}{\partial z} = 0. \quad (10\cdot5)$$

If the length of the beam is L and its depth $2d$ it follows from the form of equations (10·2) and (10·3) that in comparison with Z_z , Y_z and Y_y are of the order of magnitude of d/L and d^2/L^2 , respectively. The last two terms in equation (10·5) are thus both of the order of d^2/L^2 as compared with the first term. It therefore seems justifiable to neglect these terms in equation (10·5) in comparison with the first, and it then follows that $\partial Z_z/\partial z$ is zero. From equation (10·3), $\partial Y_z/\partial y$ is then also zero.

A similar argument in connexion with equation (10·4) shows that $\partial Z_z/\partial y$ is also zero. Remembering that on the outer surface of the beam $Y_z = 0$ and $Z_z = f_L$, it will be seen that to a close degree of approximation the shear stress Y_z is zero throughout the yielded regions and the longitudinal normal stress Z_z is equal to f_L in these regions.

A similar result is obtained if other criteria for yield, notably the Guest-Mohr hypothesis that the maximum shear stress remains constant, are assumed. The argument may be extended to include cases in which the transverse shear stress X_y exists, as, for example, in the case of a beam of circular cross-section, and also cases in which the load is distributed along the length of the beam.

11. COMBINED ELASTIC AND PLASTIC DEFORMATION

It has been postulated independently by Prandtl (1924), and Reuss (1930), that each component of strain at any point in a yielded body may be regarded as the sum of an elastic strain, calculable from the stresses in the usual way, and recoverable upon removal of the load, and a plastic strain which develops under the influence of the applied stress system in accordance with the usual laws of plastic flow (Nadai 1931). When an increment of load is applied the stresses and strains change instantaneously in accordance with the elastic laws, and the material then flows plastically in a manner governed by the changed stress system. This assumes that the increment of load causes the body to remain yielded, so that the stress components must continue to obey some criterion for yield, such as the von Mises-Hencky or Guest-Mohr law. If this condition were not fulfilled, the material would unload elastically. In many theories of plastic deformation it is assumed that the elastic components of strain can be neglected, but this assumption cannot be justified when elastic material exists in conjunction with the plastic material, as in the case of the flexure of a beam in the yield range.

As a consequence of the above considerations, the differential relations between shear stress and shear strain in a yielded body have been shown to be (Hill, Lee & Tupper 1947)

$$Gde_{yz} = dY_z + d\lambda Y_z, \quad (11.1)$$

$$Gde_{zx} = dZ_x + d\lambda Z_x, \quad (11.2)$$

$$Gde_{xy} = dX_y + d\lambda X_y, \quad (11.3)$$

G being the modulus of rigidity and λ being a non-dimensional parameter expressing the degree of plastic flow.

Suppose now that a beam, bent within the yield range, is subjected to a small torque about its longitudinal axis. In the yielded regions the shear stresses are negligibly small, so that the above equations, in particular (11.1) and (11.2), reduce to the ordinary elastic relations between shear stress and shear strain. The equation for equilibrium in the direction of the axis OZ is

$$\frac{\partial Z_x}{\partial x} + \frac{\partial Y_z}{\partial y} + \frac{\partial Z_z}{\partial z} = 0, \quad (11.4)$$

and it has been shown that $\partial Z_z/\partial z$ is negligible.

The problem of the elastic torsion of a prismatic bar is governed by the equations

$$Gde_{yz} = dY_z, \quad (11.5)$$

$$Gde_{zx} = dZ_x, \quad (11.6)$$

$$\frac{\partial Z_x}{\partial x} + \frac{\partial Y_z}{\partial y} = 0, \quad (11.7)$$

and the above argument shows that these equations also apply in the yielded regions when the applied torque is small. It therefore follows that the initial torsional rigidity for a beam bent within the yield range remains at its elastic value. A similar observation has been made by Shepherd (1948) in connexion with the torsion of a thin-walled tube strained in tension beyond the elastic limit.

the difference between the vertical scale deflexions of mirrors 1 and 2 being taken as proportional to the curvature. For the tests C and D the ratio p of the width of the elastic core of the section to the total width was calculated, the values being 0.93 and 0.60 respectively. The values of the upper and lower yield stresses deduced from the observations were 25.6 and 20.5 tons/sq.in. respectively.

The maximum torsional couple was 248 lb.in. Assuming the elastic stress distribution, the maximum shear stress induced was therefore 3.0 tons/sq.in., occurring at the centres of the longer faces of the beam, where yield had occurred in the tests C and D. There was, however, no sign of creep in the torsion readings during these tests, and on removal of the torsion loads the permanent set in twist was negligible, showing that no appreciable amount of plastic flow had occurred.

A typical set of readings during a torsion test is given in table 4 below for test C, the entries in the table being the difference between the horizontal scale deflexions for each pair of mirrors.

TABLE 4

W_2 lb.	0	1	2	3	4	5	6	7
mirrors 1-2 in.	0	0.10	0.20	0.31	0.40	0.52	0.61	0.71
mirrors 3-4 in.	0	0.09	0.19	0.29	0.39	0.51	0.58	0.69
W_2 lb.	8	9	10	11	12	13	14	0
mirrors 1-2 in.	0.80	0.91	1.01	1.11	1.23	1.33	1.44	0.01
mirrors 3-4 in.	0.78	0.88	0.98	1.10	1.20	1.29	1.40	0.00

Within the limits of accuracy of the observations the relationship between load and deflexion was linear. The ordinary statistical method of fitting a linear regression line (Fisher 1941) was therefore used to calculate the best possible estimate m of the deflexion per lb. of load, together with the variance of this estimate, treating the load as the independent variable. If s denotes the distance between each pair of mirrors and the corresponding scale, the twist occurring in the 4 in. test section between each pair of mirrors is obtained by dividing the entries in table 4 by $2s$. The torsional rigidity C was therefore $17.7(1-\eta) 2s^4/m$ lb.in.², where η denotes a small correction to the value of the applied torque due to the curvature of the specimen under load. Values of the torsional rigidity calculated in this way, together with the corresponding values of m , s and η are given in table 5.

TABLE 5

test	η %	mirrors	m (in./lb.)	s (in.)	$C \times 10^{-5}$ (lb.in. ²)	mean value of $C \times 10^{-5}$ for each test
A	0	1-2	0.1081	116.3	1.525	1.532
		3-4	0.1049	113.8	1.538	
B	1.85	1-2	0.1038	114.4	1.534	1.529
		3-4	0.1028	112.5	1.523	
C	3.94	1-2	0.1022	113.6	1.514	1.529
		3-4	0.1000	113.3	1.543	
D	5.41	1-2	0.1019	116.6	1.535	1.527
		3-4	0.1001	113.3	1.519	

The mean of the values of the torsional rigidity obtained from the two pairs of mirrors in each test is given in the final column of table 5, and it will be seen that there is very little variation between these values for the different tests. The standard error of each individual

observation of the torsional rigidity was estimated from the statistical analysis as 0.0076×10^5 , so that the standard error of the difference between any two of the mean values in the final column of table 5 is also 0.0076×10^5 (Fisher 1941). The greatest difference is between test D, in which 40 % of the cross-section had yielded, and the wholly elastic test A, this difference being only 0.33 %. The probability that this difference is due to errors of random sampling is about 50 %, so that there is no reason to suppose that the torsional rigidity changes when partial yield in bending has occurred. If in fact there is a change, it may be concluded to be extremely small.

Presuming therefore that all the eight measurements of the torsional rigidity are expected to be the same, it is possible to consider whether the experimental technique was satisfactory by examining whether these eight values show a greater degree of scatter about their general mean than would be expected from the fact that each value has a standard deviation of 0.0076×10^5 . The standard error of the deviations of these eight measurements from their general mean, obtained by summing the squares of the deviations, may be estimated as 0.010×10^5 , and although this exceeds 0.0076×10^5 the usual test of significance (Fisher 1941) shows that such a difference is well within the limits of reasonable expectation. It may therefore be concluded that there is no reason to suspect any flaws in the experimental technique and method of correcting the results which might cause greater random variations from test to test than would be expected from the standard error attributable to each observation of the torsional rigidity.

(ii) *Tests on a bar of circular cross-section*

The tests on the bar of circular cross-section, $\frac{1}{2}$ in. diameter, were carried out using similar apparatus. The length of the test piece was 10 in., the torque lever arm was 10 in. and the bending moment lever arm 11.3 in. The distance between each pair of mirrors was 6.5 in.

Five torsion tests were carried out, designated A to E. In tests A and B the beam was elastic, while during tests C, D and E the beam had partially yielded. In these latter tests the ratios of the width of the elastic core of the beam to its diameter were found from the theoretical bending moment-curvature relations to be 0.74, 0.67 and 0.61 respectively. The values of the upper and lower yield stresses were 24.0 and 18.9 tons/sq.in.

Values of the torsional rigidity C , together with the corresponding values of η , m and s are given in table 6 for each test.

TABLE 6

test	η %	mirrors	m (in./lb.)	s (in.)	$C \times 10^{-4}$ (lb.in. ²)	mean value of $C \times 10^{-4}$ for each test
A	0	1-2	0.2205	125.9	7.422	7.471
		3-4	0.2132	123.3	7.519	
B	0.29	1-2	0.2226	127.7	7.438	7.470
		3-4	0.2132	123.4	7.502	
C	0.67	1-2	0.2192	126.3	7.439	7.404
		3-4	0.2170	123.8	7.368	
D	0.71	1-2	0.2192	125.8	7.407	7.421
		3-4	0.2148	123.7	7.434	
E	0.75	1-2	0.2172	125.8	7.473	7.504
		3-4	0.2117	123.6	7.534	

The standard deviation of each individual observation of the torsional rigidity was estimated as 0.023×10^4 , but the standard deviation of each observation from their mean value, 7.454×10^4 , obtained by summing the squares of the deviations of each observation from their mean, was found to have the much higher value of 0.058×10^4 . A test of significance showed that the probability of the occurrence of such a difference due to random variations alone was only about 0.2%. It must therefore be concluded that, apart from the errors associated with the process of fitting the straight lines, a further source of error existed in these tests. Since there was a far greater variability in the results obtained from the pair of mirrors 3 and 4, it seems probable that one of the soldered attachments for these mirrors was not forming a perfectly rigid joint.

However, whether or not the observations deduced from the data taken from the pair of mirrors 3 and 4 are rejected, it is again impossible to detect any appreciable change in the torsional rigidity due to partial yield under the applied bending moment.

(b) *Bending combined with shear*

Ordinary black mild steel was again used in this experimental work. Tests were carried out on a bar of rectangular cross-section, nominal dimensions $1 \times \frac{1}{4}$ in., and a bar of nominal $\frac{3}{8}$ in. square cross-section. The apparatus was similar for both series of tests, and was as shown diagrammatically in figure 36.

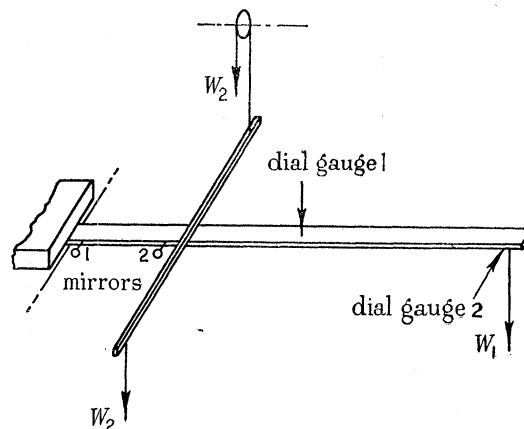


FIGURE 36. Apparatus for torsion tests on a cantilever.

The bars were tested as cantilevers, of length 25 in., the $1 \times \frac{1}{4}$ in. bar being bent about its weaker principal axis. At the encastered end the bars were rigidly clamped by means of a 1 in. plate bolted to a heavy base plate by eight $\frac{3}{8}$ in. bolts. The vertical deflexion of the beam was measured at mid-span by a Mercer dial gauge of the plunger type, reading to the nearest 0.0001 in. This position for the measurement of the deflexion was chosen because the total travel of the plungers on these gauges is $\frac{1}{2}$ in., and the end deflexion of each beam was somewhat greater than this.

A torque could be applied to the beam near the encastered end through a light loading lever, clamped to the beam 6 in. from the encastered end, the lever arm for the torsion loads being 13 in. The twist of the beam was measured in the usual way by the two mirrors, 1 and 2, fixed to short lengths of copper wire soldered to the beam at points $\frac{1}{2}$ and $5\frac{1}{2}$ in. from the encastered end of the beam.

A small correction to the applied torque was due to the fact that the free end of the beam deflected slightly in a lateral direction when the torque was applied. This lateral deflexion δ_2 was measured by dial gauge 2, as shown, the correction to the applied torque being $W_1 \delta_2$.

Five torsion tests were carried out on each beam, designated A to E in each case. In each test the load W_1 was held constant while the torsion loads W_2 were increased in 1 lb. increments from 0 to 10 lb. and then removed. It was found that the vertical deflexion changed very little during the torsion tests even when the beams had partially yielded, so that it was possible to proceed with the flexure after the completion of each torsion test.

Using the theory of flexure of a cantilever in the yield range as given by Baker & Roderick (1940), the readings of dial gauge 1 for each value of W_1 could be analyzed to find the values of the upper and lower yield stresses giving the best degree of fit with the observations of load and deflexion during flexure in the yield range. For the $1 \times \frac{1}{4}$ in. beam these values were 20.9 and 18.1 tons/sq.in., and for the $\frac{3}{8}$ in. square beam 20.7 and 17.7 tons/sq.in. respectively.

For each beam the torsion tests A and B were carried out while the beam was still elastic, whereas in tests C, D and E, the beams had partially yielded. The shape of the boundary between the elastic core of the beams and the outer yielded regions was calculated for these latter tests, and the results of these calculations are given in figure 37.

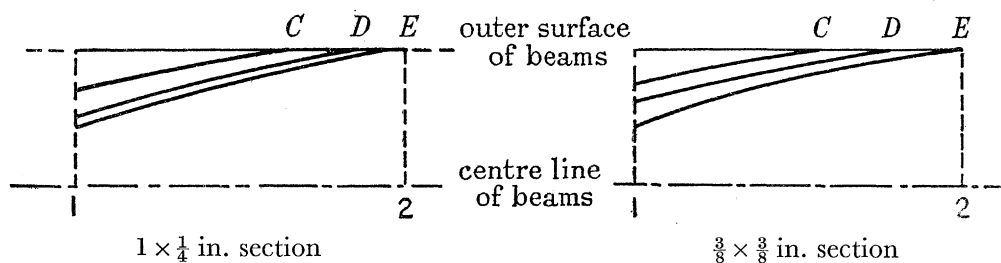


FIGURE 37. Shape of elastic-plastic boundaries. The numbers refer to the mirrors.

The maximum torque applied during each torsion test was 130 lb.in., subject to the small correction already described. The maximum shear stress induced by this torque, assuming the elastic stress distribution, was 3.2 tons/sq.in. for the beam of $1 \times \frac{1}{4}$ in. cross-section, occurring at the centres of the longer sides, where yield due to the bending stresses occurred. For this beam there was no sign of creep of the mirror readings during the torsion tests, and when the loads were removed the permanent set in twist was zero within the limits of experimental error, indicating that no plastic flow in torsion had occurred.

The maximum shear stress in the beam of $\frac{3}{8}$ in. square cross-section was 4.9 tons/sq.in., occurring at the centre of each side. For this beam creep of the mirror readings was observed during the torsion tests D and E, at loads of 8 and 6 lb. respectively, and on removing the torsion loads it was noticed that a small residual twist remained in the test section. This indicated that plastic flow in torsion had occurred in these tests, presumably due to the somewhat higher value of the maximum shear stress. The readings taken during these tests are given in table 7, the entries in this table being the difference between the vertical scale deflexions for the mirrors 1 and 2.

The observations were analyzed as described previously, and the results of the tests on the $1 \times \frac{1}{4}$ in. beam are summarized in table 8.

YIELDED MILD STEEL BEAMS

225

TABLE 7

W_2 (lb.)	0	1	2	3	4	5	6	7	8	9	10	0
test D	0	0.50	1.01	1.50	1.99	2.50	3.00	3.52	4.04*	4.58	5.08	0.05
test E	0	0.52	1.04	1.55	2.05	2.55	3.08*	3.59	4.14	4.68	5.24	0.10

* Creep observed.

TABLE 8

test	m (in./lb.)	s (in.)	η (%)	$C \times 10^{-4}$ (lb.in. ²)
A	0.3341	131.6	0	5.120
B	0.3324	130.8	0.16	5.107
C	0.3298	130.2	0.72	5.095
D	0.3325	131.4	0.93	5.090
E	0.3285	131.1	1.00	5.136

It will be seen that the observations of the torsional rigidity vary very little from a mean value of 5.110×10^4 , and in fact the highest value of the rigidity occurred in test E, in which the beam was most plastic. The standard error of each observation of the torsional rigidity was estimated from the data as 0.016×10^4 . The standard error of the difference between any two of the torsional rigidities was therefore $0.016 \times 10^4 \sqrt{2}$, or 0.022×10^4 . The greatest difference occurring was 0.041×10^4 between tests C and E, and a test of significance showed that the probability of this difference being due to errors of random sampling was about 7.5%. This probability is low, but cannot be judged significant.

Each observation of the torsional rigidity may therefore be expected to be the same, and their degree of scatter about their general mean, 5.110×10^4 , may be examined to form a separate estimate of their standard error. In this way, the standard error may be estimated as 0.019×10^4 , and this value does not differ significantly from the previous value 0.016×10^4 . Thus the only cause of variance of the observations was that associated with the process of estimating the slopes of the straight lines fitted to the observations of load and deflexion. The experimental technique was therefore satisfactory.

The results of the tests on the $\frac{3}{8}$ in. square section beam are summarized in table 9. In analyzing the results of the torsion tests D and E, in which creep occurred, the observations taken after creep was first noted, as indicated in table 7, were rejected.

TABLE 9

test	m (in./lb.)	s (in.)	η (%)	$C \times 10^{-4}$ (lb.in. ²)
A	0.5066	132.6	0	3.403
B	0.5065	132.6	0.12	3.399
C	0.5015	132.4	0.32	3.421
D	0.5012	132.6	0.36	3.426
E	0.5100	134.1	0.42	3.404

As in the previous tests, there is no marked variation in the values of the torsional rigidity from their mean value, 3.411×10^4 . The standard errors of the rigidities associated with the process of fitting a straight line through the observations taken in each test were

tests A, B and C, 0.0056×10^4 , test D, 0.0090×10^4 , test E, 0.0140×10^4 ,

the higher values in tests D and E being due to the smaller number of observations available. The standard error as deduced from the deviations of each value of the torsional rigidity

from their mean is 0.0121×10^4 , and this value does not differ significantly from those given above. The experimental technique was therefore again satisfactory.

The results of these tests, both on beams in pure bending and with bending combined with shear, confirm that the initial torsional rigidity remains unaltered at its elastic value when partial yield has occurred. The latter tests also verify indirectly that when a beam is bent in the yield range the shear is carried entirely in the central elastic core of the beam.

PART III. THE CONDITIONS CAUSING LATERAL INSTABILITY

13. INTRODUCTION

If a thin deep beam is loaded in one plane so as to cause flexure about the stronger, or primary principal axis of its cross-section, failure by lateral buckling may occur by the development of lateral deflexions out of the plane of the applied loads, together with twist about the longitudinal axis of the beam. Prediction of the conditions causing lateral buckling was shown in part I to involve a knowledge of the initial secondary flexural rigidity B , and the initial torsional rigidity C . B may be defined as the initial slope of the bending moment-curvature relation for flexure about the weaker, or secondary principal axis of the cross-section of the beam, while the applied loads are held constant, and a corresponding definition may be given for C .

In this part the conditions causing lateral instability for mild steel beams of rectangular cross-section are discussed, it being assumed that the applied loads are sufficiently great to cause partial yield of the beams. In part I a discussion of the flexure of partially yielded beams of annealed mild steel was given. For such steel the stress-strain characteristic may be taken as identical for tension and compression until strain hardening sets in. Hooke's Law is obeyed until the upper yield stress μf_L is reached, after which further straining takes place at a constant lower yield stress f_L up to the point where strain hardening commences.

It was shown in part I how the initial secondary flexural rigidity falls off progressively as the bending moment is increased in the yield range, and in part II the initial torsional rigidity was shown to remain constant at its value for elastic torsion. Using these results the criterion for lateral instability is determined for beams bent by pure terminal couples, and experimental verification of the results is given. A finite difference approximation method is also developed to cover cases in which the bending moment varies linearly along the beam, and is applied to the case of a beam with a central concentrated load, and also a cantilever.

14. PURE BENDING

The critical lateral buckling moment for a beam bent by pure terminal couples depends on the degree of fixity of the ends of the beam. If it is supposed that the ends are free to rotate about the axis of secondary bending but are prevented from twisting about the longitudinal axis of the beam, the critical lateral buckling moment is given by

$$M_{cr} = \frac{\pi}{L} \sqrt{\left(\frac{BC}{\left(1 - \frac{B}{A}\right) \left(1 - \frac{C}{A}\right)} \right)}, \quad (14.1)$$

where L is the length of the beam, and A , termed the overall primary flexural rigidity, is the ratio of the primary bending moment to the primary curvature. This result may readily be derived by the method indicated by Reissner (1904) for the case of a cantilever, and differs from the result usually given by the inclusion of the two terms in the denominator beneath the radical.

If the beam is of breadth $2b$ and depth $2d$, d being greater than b , the elastic flexural rigidities A_E and B_E about the primary and secondary principal axes are $\frac{4}{3}Ebd^3$ and $\frac{4}{3}Edb^3$, respectively, E being Young's modulus. The torsional rigidity C is given by $\frac{1}{3}Gdb^3f(b/d)$, G being the modulus of rigidity, where $f(b/d)$ is given closely by $(1 - 0.63b/d)$. The bending moment M_Y at which yield first occurs in the outer fibres of the beam is given by $\frac{4}{3}\mu f_L bd^2$. Equation (14.1) may therefore be rewritten in non-dimensional form as

$$\frac{L}{2d} = \pi \frac{\sqrt{(EG) M_Y b^2 A}}{\mu f_L M_{cr} d^2 A_E} \sqrt{\left\{ \frac{\frac{B}{B_E} f\left(\frac{b}{d}\right)}{\left(\frac{A}{A_E} - \frac{B}{B_E} \frac{b^2}{d^2}\right) \left(\frac{A}{A_E} - 4 \frac{G}{E} f\left(\frac{b}{d}\right) \frac{b^2}{d^2}\right)} \right\}}. \quad (14.2)$$

As stated in part I, the relation between the bending moment and curvature during primary flexure in the yield range is

$$\frac{M_{cr}}{M_Y} = 1 + (1 - p^2) \left(\frac{3}{2\mu} - 1 \right), \quad \frac{\kappa_1}{\kappa_Y} = \frac{1}{p}, \quad (14.3)$$

where the depth of the central elastic portion of the beam is $2pd$, κ_1 is the curvature, and κ_Y is the curvature corresponding to M_Y . The overall primary flexural rigidity is therefore given by

$$A = \frac{M_{cr}}{\kappa_1} = p A_E \frac{M_{cr}}{M_Y}. \quad (14.4)$$

When the curvature becomes infinite, so that $p = 0$, the beam becomes fully plastic, and is sustaining the greatest possible bending moment on this theory. It will be seen from equation (14.3) that the value M_p of this moment, termed the fully plastic moment, is $3/2\mu$. In practice, however, the theory breaks down for large curvatures owing to the onset of strain hardening in the outer fibres.

Illustrative calculations have been made using the following numerical values:

$$E = 30 \times 10^6 \text{ lb./sq.in.}, \quad G = 12 \times 10^6 \text{ lb./sq.in.}, \\ \mu f_L = 20 \text{ tons/sq.in.}, \quad b/d = \frac{1}{8}, \quad f(b/d) = 0.92,$$

so that equation (14.2) reduces to

$$\frac{L}{2d} = 20.8p \sqrt{\left\{ \frac{\frac{B}{B_E}}{\left(\frac{A}{A_E} - \frac{1}{64} \frac{B}{B_E}\right) \left(\frac{A}{A_E} - 0.023\right)} \right\}}. \quad (14.5)$$

From equations (14.3), (14.4), and (14.5), relations between $L/2d$ and M_{cr}/M_Y were calculated for values of μ between 1.0 and 1.5, B/B_E being known as a function of p from the results of part I. These relations are shown in figure 38, together with the rectangular hyperbola appropriate to wholly elastic flexure.

It will be seen that as the value of M_{cr}/M_Y for a given value of μ increases above 1 the corresponding value of $L/2d$ decreases at first more rapidly than if the section had remained elastic. A sharply defined minimum value of $L/2d$ is eventually reached, after which the value of $L/2d$ rapidly tends to infinity as M_{cr} approaches the fully plastic moment M_p . This latter branch of the curve is of little interest, however, since a beam of given length will always buckle laterally when the bending moment assumes the somewhat smaller critical value given by the lower branch of the curve.

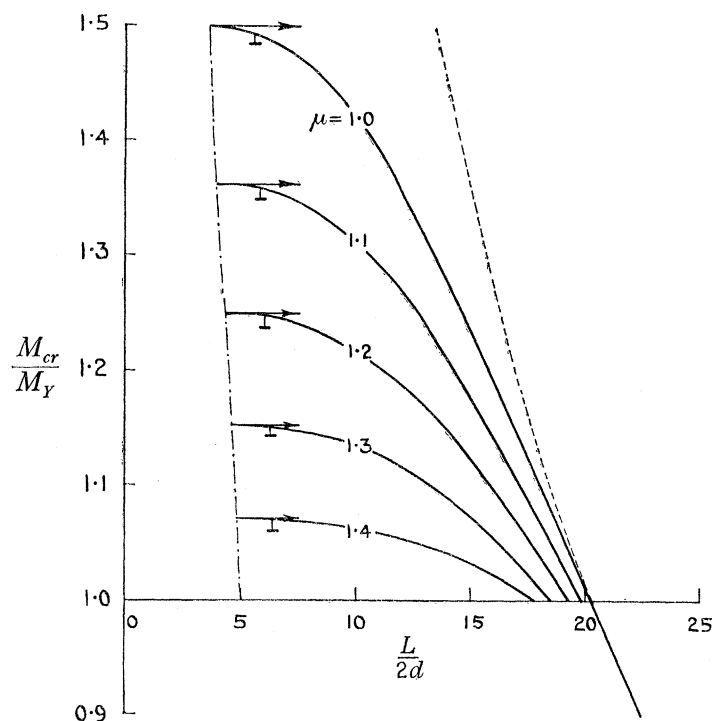


FIGURE 38. The critical lateral buckling moment for a beam in pure bending. \perp points where $\kappa_1/\kappa_Y = 8$; — — — locus of minima of $L/2d$; - - - relation assuming elastic behaviour.

The discrete drop in the value of B at the onset of plasticity, discussed in part I, causes a discrete drop in the value of $L/2d$ at $M_{cr} = M_Y$ for values of μ greater than 1. Lateral buckling may therefore be expected to occur rather abruptly in certain cases. As an example, consider a beam for which $L/2d = 17.5$, $\mu = 1.4$. From figure 38 it will be seen that when the applied primary bending moment M_1 is just less than M_Y , $M_{cr} = 1.16 M_Y$, since the section is entirely elastic, whereas when M_1 is just equal to M_Y , $M_{cr} = M_Y$.

The equation to the locus of the minima of $L/2d$ may readily be determined, since the value of p at the minima is of the order of 0.1 for any value of μ . It was shown in § 5, part I, that if p is less than a certain critical value, depending on μ , the unloading zones which form during the secondary flexure process are triangular in shape. This point is illustrated in figure 7, from which it will be seen that the critical value of p is never less than $\frac{1}{3}$. Thus at the minima of $L/2d$ the unloading zones are always triangular, and reference to equation (5.8), part I, shows that in this case $B/B_E = kp$, where k is a function of μ alone. Thus in equation (14.2), $L/2d$ is given explicitly as a function of p in the neighbourhood of the minima. Differentiating this equation, it is found that the value of p corresponding to the minimum

value of $\frac{L}{2d}$ is approximately $\frac{16\mu G b^2}{3 E d^2} f\left(\frac{b}{d}\right)$, p^2 being neglected in comparison with unity. With this approximation it then follows that the locus of the minima of $L/2d$ is given by

$$\left(\frac{L}{2d}\right)_{\min} = \frac{8\pi G b^3}{3 f_L d^3} f\left(\frac{b}{d}\right) / \sqrt{\left(\frac{3}{2\mu k} - \frac{b^2}{d^2}\right)}, \quad (14.6)$$

and this locus is plotted in figure 38.

As discussed previously in part I, the analysis of flexure in the yield range breaks down when the primary bending moment is large enough to induce strain hardening in the outer fibres of the beam. This occurs when the extreme fibre strain is about eight times the strain at yield, so that $\kappa_1/\kappa_Y = 1/p = 8$. The points at which the value of p is $\frac{1}{8}$ are marked on the curves in figure 38. It will be seen that the minima of $L/2d$ are closely approached along the lower branches of the curves before the value of p falls from 1 at the onset of plasticity to $\frac{1}{8}$. Since as already discussed it is only the lower branches of the curves that are of interest, there is little point in extending the analysis to include the effects of strain hardening.

15. BENDING COMBINED WITH SHEAR

(a) The governing differential equation

In the case of a beam loaded in such a way that a constant shear force exists, so that the bending moment varies linearly along the length of the beam, it is not possible to give an explicit solution for the critical lateral buckling moment. It has been shown by Federhofer (1931) that the differential equation governing this class of problem is

$$\frac{1}{P^2} \frac{d}{ds} \left[\frac{AB}{(A-B)s} \frac{d}{ds} \left(C \frac{d\phi}{ds} \right) \right] + \left(1 - \frac{C}{A} \right) s \frac{d\phi}{ds} + \phi = 0, \quad (15.1)$$

where P is the shear force, ϕ is the angle of twist of the beam measured from its unloaded position, and s denotes distance measured along the axis of the beam. The relation between ϕ and the curvature κ_2 about the secondary principal axis is

$$\frac{d}{ds} \left(C \frac{d\phi}{ds} \right) = \left(1 - \frac{B}{A} \right) P \kappa_2 s, \quad (15.2)$$

and the origin of s is chosen so that the primary bending moment M_1 is Ps .

In general there will exist three independent end conditions which will enable the critical load causing lateral instability to be determined, since equation (15.1) is of the third order. Two particular cases are considered, as indicated in figures 39 and 40.

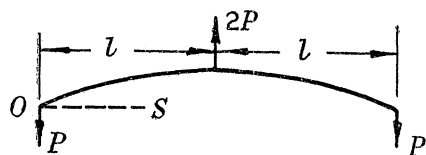


FIGURE 39. Central concentrated load.

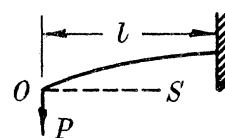


FIGURE 40. Cantilever.

Figure 39 illustrates the case of a beam of length $2l$ subjected to a central concentrated load $2P$. It is assumed that at each end of the beam twist is prevented, but that there is freedom to rotate about the secondary principal axis. When $s = 0$, $\phi = 0$, and from equation (15.2), $d^2\phi/ds^2 = 0$. At the centre of the beam, where $s = l$, $d\phi/ds = 0$ by symmetry.

Figure 40 illustrates the case of a cantilever of length l subjected to an end load P . At the free end the torque is zero, so that when $s = 0$, $d\phi/ds = 0$. At the encastered end, $\phi = 0$ and the secondary curvature κ_2 is also zero, so that from equation (15.2), $d^2\phi/ds^2 = 0$. In both these cases the load is assumed to be applied through the centroid of the cross section.

Before proceeding to the solution of equation (15.1) it will be convenient to rewrite this equation in non-dimensional form. Making the substitutions

$$s = xl, \quad \gamma^2 = \frac{P^2 l^4}{B_E C} \left(1 - \frac{B_E}{A_E}\right),$$

it is found that
$$\frac{1}{\gamma^2} \frac{d}{dx} \left[F(x) \frac{1}{x} \frac{d^2\phi}{dx^2} \right] + \frac{d}{dx} (x\phi) = \frac{C}{A} x \frac{d\phi}{dx}, \quad (15.3)$$

where
$$F(x) = \frac{(1 - B_E/A_E) B}{(1 - B/A) B_E}.$$

When the applied load is sufficiently great to ensure that yield occurs in some length of the beam, the function $F(x)$ varies with x in this region, since as discussed in part I both A and B are functions of the primary bending moment and therefore of x when the beam has partially yielded. For flexure in the yield range $F(x)$ cannot be expressed in a manner suitable for differentiation, so that it is necessary to integrate equation (15.3), giving

$$F(x) \frac{d^2\phi}{dx^2} + \gamma^2 x^2 \phi = \gamma^2 f_a(x), \quad (15.4)$$

where
$$f_a(x) = \frac{C}{A_E} x \int_a^x \frac{A_E}{A} x d\phi.$$

By considering the end conditions it will be seen that the arbitrary constant of integration a assumes the value 0 for the case of a central concentrated load, and 1 for the case of a cantilever. The utility of equation (15.4) lies in the fact that C/A_E is usually small. With the numerical values adopted for the case of pure bending, $C/A_E = 0.023$. The term $f_a(x)$ is therefore small, and can be estimated with sufficient accuracy from a rough guess of the mode of ϕ .

(b) Solution by finite difference approximations

The eigen-value γ in equation (15.4) may readily be determined by using finite difference approximations to the first and second derivatives of ϕ . The work was facilitated by the use of the method described by Fox (1947). In this method a preliminary estimate of the mode is formed by neglecting all but the first, dominant, term in the infinite series of finite differences for the derivatives. From this mode numerical values of the subsequent terms in the series are calculated, and these values are then incorporated to form an improved estimate of the mode and eigen-value. The process may be repeated until the desired accuracy is obtained, but it is a feature of this method that rapid convergency is secured.

The unit length of the beam subjected to a constant shearing force is divided into n equal parts of length $1/n$ by a series of points numbered 0 to n , the point 0 coinciding with the origin

of s . Following the scheme adopted by Fox (Tables 1942), the finite differences are computed as follows:

$$\begin{array}{ccccccc} \phi_{r-1} & & \delta''_{r-1} & & & & \\ & \delta'_{r-\frac{1}{2}} & & & & & \\ \phi_r & & \delta''_r & \text{etc.} & \delta'_r = \frac{1}{2}(\delta'_{r-\frac{1}{2}} + \delta'_{r+\frac{1}{2}}) & \text{etc.} & \\ & \delta'_{r+\frac{1}{2}} & & & & & \\ \phi_{r+1} & & \delta''_{r+1} & & & & \end{array}$$

The derivatives of ϕ at the point r are given by

$$\left(\frac{d\phi}{dx}\right)_r = n[\delta'_r - \frac{1}{6}\delta'''_r + \frac{1}{30}\delta^v_r \dots], \quad (15.5)$$

$$\left(\frac{d^2\phi}{dx^2}\right)_r = n^2[\delta''_r - \frac{1}{12}\delta^{iv}_r + \frac{1}{90}\delta^{vi}_r \dots]. \quad (15.6)$$

Replacing $d^2\phi/dx^2$ in equation (15.4) by its finite difference approximation (15.6) gives

$$\phi_{r-1} = \left[2 - \frac{\gamma^2 r^2}{n^4 F(r)}\right] \phi_r - \phi_{r+1} + \frac{\gamma^2 f_a(r)}{n^2 F(r)} + \Delta, \quad (15.7)$$

where $\Delta = \frac{1}{12}\delta^{iv}_r - \frac{1}{90}\delta^{vi}_r \dots$

The term Δ in equation (15.7) represents the 'difference correction' of Fox (1947) which is calculated numerically from the preliminary estimate of the mode and used to improve the estimate of the mode and eigen-value.

(c) *Beam with central concentrated load*

To illustrate the method, consider the case of a beam with a central concentrated load, applied through the centroid of the cross section. At the centre of the beam, at the point $r = n$, $d\phi/dx = 0$, so that

$$\frac{1}{2}(\phi_{n+1} - \phi_{n-1}) - \frac{1}{6}\delta'''_n + \frac{1}{30}\delta^v_n \dots = 0. \quad (15.8)$$

The procedure adopted is to form a preliminary estimate of the mode by neglecting the difference corrections and guessing the mode of ϕ to form a rough estimate of the value of $f_0(x)$ in equation (15.7). Assigning to ϕ_n an arbitrary value, say 10^6 , and guessing a value for γ , ϕ_{n-1} may be calculated from equation (15.7), with $r = n$, and equation (15.8), by eliminating the value ϕ_{n+1} which is exterior to the length of the beam under consideration. ϕ_{n-2} , ϕ_{n-3} , etc., may then be calculated in succession from equation (15.7) with $r = n-1$, $n-2$, etc., until finally a value of ϕ_0 is obtained. This value should be zero; if it is not, a fresh value of γ must be guessed and the process repeated.

In this way a preliminary estimate of the mode of ϕ is formed. This estimate is then used to calculate the values of $f_0(x)$ and the difference corrections, and with these values incorporated in equations (15.7) and (15.8) the process is repeated to form a closer estimate of the mode and the eigen-value γ . The convergency of the method is such that this second estimate of γ is usually of great accuracy.

Calculations were carried out for a beam for which $b/d = \frac{1}{8}$, with numerical values of E , G , and μf_L as used in the case of pure bending. If M_{cr} denotes the maximum bending moment existing at the centre of the beam when lateral buckling occurs, it may readily be shown that

$$\frac{L}{2d} = 12.80\gamma \frac{M_Y}{M_{cr}}, \quad (15.9)$$

where L denotes the total length of the beam, $2l$. The value of γ corresponding to wholly elastic behaviour is found from the solution of Federhofer (1931) to be 2.128.

The value of n chosen for the calculations was usually 20, and in a few cases 40. These values may appear to be unduly large, particularly as the primary purpose of the development of the finite difference correction method was to reduce the size of the interval necessary to obtain an accurate result. The reason for this choice is that since the bending moment varies linearly along the length of the beam, only a comparatively small central portion actually yields, and it was desired to include a reasonable number of points in the yielded region, where the flexural rigidities A and B become functions of the bending moment. Since at any section the value of primary bending moment M_1 is xM_{cr} , the value x_0 of x at which the yielded region commences is M_Y/M_{cr} , M_Y being the bending moment at which yield first occurs. Since the maximum bending moment which the section can sustain is the fully plastic moment $\frac{3}{2}M_Y/\mu$, x_0 can never be less than $\frac{2}{3}\mu$, so that even when μ is unity only one third of the length of the beam yields.

To illustrate the method, consider a particular case for which $\mu = 1.1$, $M_{cr}/M_Y = 1.143$. As shown in part I, the value of B drops by a discrete amount when the primary bending moment M_1 attains the value M_Y at which yield just occurs. It was thought that the finite difference approximations would be most accurate if this discontinuity in the value of B was arranged to take place at the centre of an interval, and for this case, $M_1 = M_Y$ when $x = 0.875$, midway between the points $r = 17$ and $r = 18$.

Values of $F(x)$, calculated in accordance with the theory given in part I, are given in table 10, together with the values of A/A_E required for the calculation of $f_0(x)$.

TABLE 10

x	0.9	0.95	1.0
$F(x)$	0.928	0.869	0.798
A/A_E	0.988	0.949	0.890

In the first stage of the calculations the finite difference corrections in equations (15.7) and (15.8) were neglected. The value of $f_0(x)$ was calculated by assuming the mode of ϕ calculated for $\mu = 1.1$, $M_{cr}/M_Y = 1.290$.

The first value of γ assumed was 2.07, giving $\phi_0 = -8143$. The second value of γ assumed was 2.0609, giving $\phi_0 = -278$. The mode thus obtained was considered to be sufficiently accurate to enable the finite difference corrections to be calculated, and a fresh estimate of $f_0(x)$ to be made. Table 11 gives this mode, together with the finite differences δ' , δ'' , δ''' and δ^{iv} , and the estimate of $f_0(x)$.

A fresh calculation was now made using the values of $f_0(x)$ and the finite differences given in table 11. It was necessary to assume some values of the finite differences, and these assumed values are shown in brackets in the table. The finite differences δ^v , δ^{vi} , etc., were found to be negligible.

The first value of γ assumed was 2.0609, giving $\phi_0 = 2969$. The next value assumed was 2.0643, giving $\phi_0 = -58$, and interpolating from these values γ is found to be 2.0642. The inclusion of the finite difference corrections and improved estimate of $f_0(x)$ therefore changed the eigen-value by only 0.16%, so that no further improvement was necessary.

The calculation for $\gamma = 2.0643$, following equations (15.7) and (15.8), is set out in detail in table 12.

YIELDED MILD STEEL BEAMS

233

TABLE 11

r	ϕ	δ'	δ''	δ'''	δ^{iv}	$f_0(x)$
20	1,000,000			(-2,185)		
		6,586		(-2,112)	(-147)	9,639
19	993,414		-10,841	(-2,038)	(-147)	9,004
		17,427		-1,891		
18	975,987		-8,950	-1,744	-147	8,187
		26,377		-1,744		
17	949,610		-7,206	-1,049	-695	7,277
		33,583		-1,049		
16	916,027		-6,157	-981	-68	6,338
		39,740		-981		
15	876,287		-5,176	-898	-83	5,411
		44,916		-898		
14	831,371		-4,278	-808	-90	4,527
		49,194		-808		
13	782,177		-3,470	-712	-96	3,707
		52,664		-712		
12	729,513		-2,758	-617	-95	2,967
		55,422		-617		
11	674,091		-2,141	-522	-95	2,317
		57,563		-522		
10	616,528		-1,619	-435	-87	1,759
		59,182		-435		
9	557,346		-1,184	-349	-86	1,292
		60,366		-349		
8	496,980		-835	-274	-75	912
		61,201		-274		
7	435,779		-561	-208	-66	613
		61,762		-208		
6	374,017		-353	-148	-60	387
		62,115		-148		
5	311,902		-205	-100	-48	224
		62,320		-100		
4	249,582		-105	-61	-39	115
		62,425		-61		
3	187,157		-44	-31	-30	48
		62,469		-31		
2	124,688		-13	-11	-20	14
		62,482		-11		
1	62,206		-2		(-10)	2
		62,484				
0	-278				(0)	0

TABLE 12. $\phi_{20}=10^6$, $\phi_{19}=993,735$

$r-1$	$-\frac{1}{F(r)}\left(\frac{\gamma r}{400}\right)^2$	$\left(\frac{\gamma}{20}\right)^2 \frac{f_0(r)}{F(r)}$	$\frac{1}{12}\delta_r^{iv}$	ϕ_{r-1}
18	-10,995	110	-12	976,573
17	-9,081	94	-12	950,412
16	-7,315	78	-58	916,956
15	-6,252	68	-6	877,310
14	-5,257	58	-7	832,458
13	-4,346	48	-8	783,300
12	-3,526	39	-8	730,647
11	-2,802	32	-8	675,216
10	-2,176	25	-8	617,616
9	-1,645	19	-7	558,383
8	-1,205	14	-7	497,952
7	-849	10	-6	436,676
6	-570	7	-6	374,831
5	-359	4	-5	312,626
4	-208	2	-4	250,211
3	-107	1	-3	187,687
2	-45	1	-3	125,116
1	-13	0	-2	62,530
0	-2	0	-1	-58

The results of the calculations are presented in figure 41, in which the relations between $L/2d$ and M_{cr}/M_Y are plotted for values of μ from 1.0 to 1.4.

A comparison of the curves in figure 41 with those of figure 38 shows that the effect of yield is much less marked than in the case of pure bending, owing to the fact that with a central concentrated load yield is confined to a comparatively short central section. In contrast to the case of pure bending, the curves terminate at a finite minimum value of

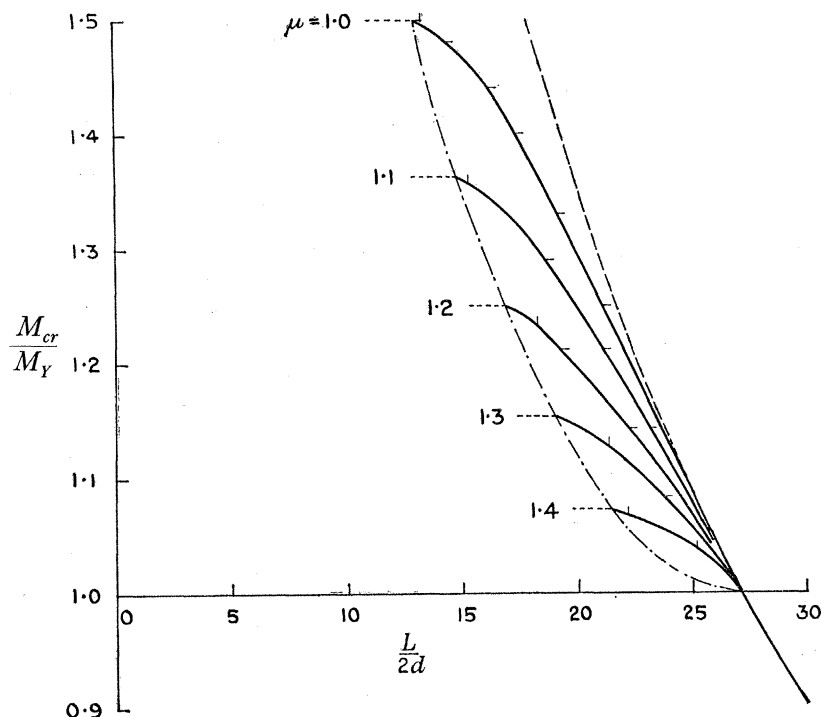


FIGURE 41. Lateral buckling of a beam with a central concentrated load. — points calculated with $n=20$; | points calculated with $n=40$; — locus of minima of $L/2d$; — relation assuming elastic behaviour; ---- fully plastic moments.

$L/2d$ as the central bending moment reaches the fully plastic moment. An investigation of the nature of the limit as μ approaches the value 1.5 shows that the locus of the minima of $L/2d$ terminates on the elastic line when $M_{cr} = M_Y$. As already pointed out, the theory breaks down before the fully plastic moment is reached, owing to the onset of strain hardening, but this only happens when κ_1/κ_Y is about 8 and the bending moment is within 0.5% of the fully plastic moment.

(d) Cantilever

Calculations similar to those just described were carried out for the case of a cantilever with a concentrated load applied at the free end through the centroid of the cross-section. The ratio of b/d was again chosen as $\frac{1}{8}$, and the values of E , G , and μf_L were as previously given. If the length of the cantilever is L , it follows that

$$\frac{L}{2d} = 6.40\gamma \frac{M_Y}{M_{cr}}. \quad (15.10)$$

The value of γ for the case in which the cantilever remains elastic was shown by Reissner (1904) to be 4.090.

A calculation with $n = 20$ for the case in which $\mu = 1.0$ and the bending moment at the encastered end was equal to the fully plastic moment gave the value 3.980 for γ , so that the reduction in $L/2d$ as compared with the value calculated on the assumption of elastic behaviour was only 2.7%. The small effect of yield in this case is due to the fact that the reduction in B occurs near the encastered end of the beam, where the angle of twist, and consequently the secondary bending moment, is small.

16. EXPERIMENTAL WORK

Owing to the difficulty of obtaining suitable specimens of steel strip of sufficient length, the experimental work was restricted to the case of pure bending, which of all the cases considered involved the use of the shortest specimens. The material used was bright drawn mild steel strip, of nominal dimensions $1 \times \frac{1}{8}$ in. The dimensions of this strip varied very little along the length of each specimen, the width being maintained within ± 0.0003 in. and the depth within ± 0.0006 in. It was therefore not necessary to machine the specimens to size.

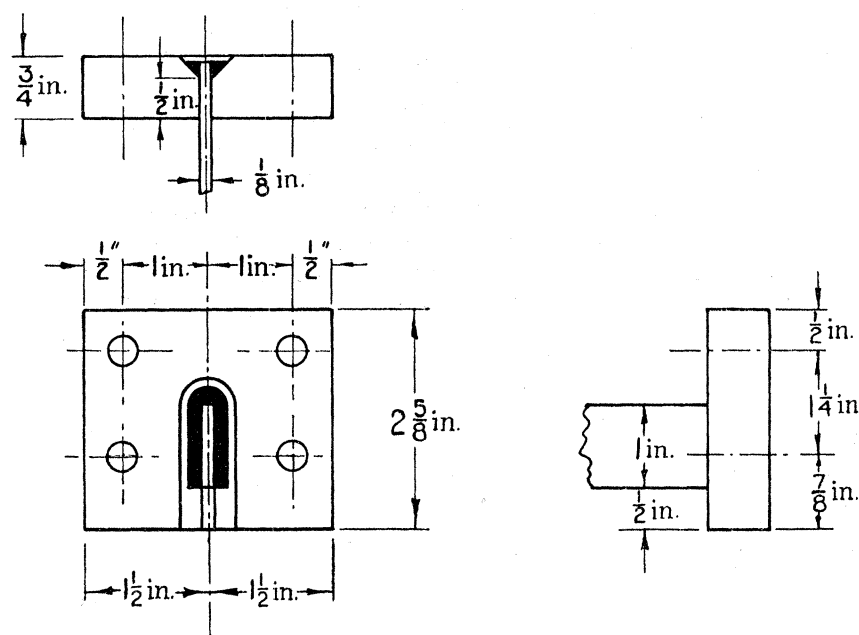


FIGURE 42. Encastering block.

The ends of each specimen were prevented from twisting by means of encastering blocks. Each block consisted of a $3 \text{ in.} \times 2 \frac{5}{8} \text{ in.}$ steel block, $\frac{3}{4} \text{ in.}$ thick, in which a slot was sawn by an $\frac{1}{8} \text{ in.}$ saw cutter, as shown in figure 42. Since the strip was about 0.002 in. oversize in width, the ends of the specimens were very good force fits in the slots. On the back face of each block the slot was milled out to form a V, into which the end of the specimen protruded. A run of weld was then made round this V to secure the specimen to the block.

Four clearance holes for $\frac{3}{8} \text{ in.}$ bolts were drilled in each block, thus enabling the block to be bolted into the end fittings described in part I. Figure 43 shows a specimen bolted in position in the end fittings, the bolts being located in such a way that the centre line of the specimen passed through the horizontal axes of the ball races visible in the figure. Application of equal vertical loads at the ends of the loading levers therefore caused a uniform bending

moment to be applied along the length of the specimen about its stronger, or primary principal axis. The specimen was free to rotate at each end about the secondary principal axis, while twist at each end was prevented by the encastering blocks.

The primary curvature was measured during each test by the two dial gauges which can be seen in figure 43. These gauges were of the standard spring-loaded plunger type, reading to the nearest 0.0001 in., and measured the vertical deflexion of each loading lever. The central angle of twist was also measured by means of a small plane mirror attached to a short length of copper wire soldered to the specimen, a scale with $\frac{1}{10}$ in. graduations being viewed through a telescope by reflexion from this mirror. The distance between the mirror and the scale was 10 ft.

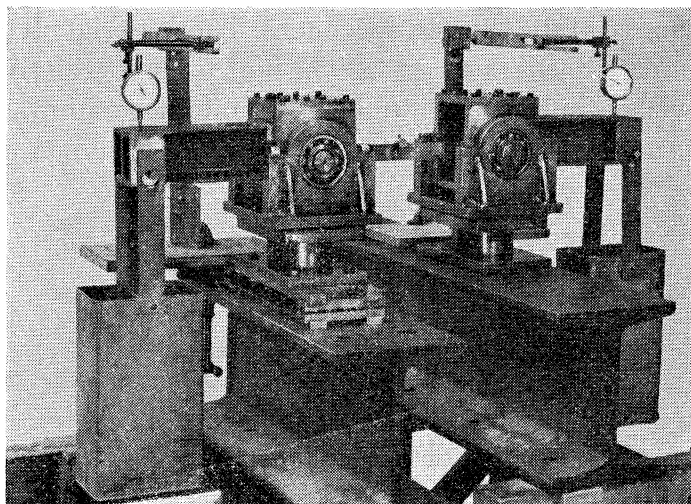


FIGURE 43

Two stocks of the bright-drawn strip, designated A and B, were available for the tests, and analyses of two samples taken from each stock were made. The results of these analyses are given in table 13, from which it will be seen that the composition of the steel was somewhat variable. Unfortunately, however, no better material was available.

TABLE 13. PERCENTAGE COMPOSITION OF SAMPLES

sample	C	Si	Mn	Ni	Cr	P	S
A	0.22	0.13	0.59	nil	0.02	0.05	0.05
	0.27	0.12	0.60	nil	0.02	0.05	0.05
B	0.15	0.24	0.61	nil	0.02	0.03	0.05
	0.14	0.13	0.62	nil	0.02	0.03	0.04

Before heat treatment, the specimens were straightened by cold bending, and then clamped together in a jig. The annealing was carried out in sealed steel tubes filled with an inert atmosphere of argon. The soaking temperature was 910° C, and the cooling rate was such that the temperature dropped to 200° C in 110 min. On removal from the jig the specimens were still distorted to some extent, and preliminary tests showed that the imperfections were such that considerable lateral deflexion and twist developed at an early stage in the tests.

This rendered observation of the critical buckling moment very difficult. The critical moment is, by definition, the moment at which lateral deflexion and twist develop in

an initially straight beam. In a test the departures from straightness during flexure in the yield range must not become so excessive that the stress distribution differs materially from that due to the primary bending moment alone, for if this is the case the secondary flexural rigidity will no longer be calculable from the primary bending moment alone.

The device adopted to overcome this difficulty was to tilt one of the end fittings through a small angle by means of a wedge at one side of its base, thus introducing a further imperfection in the form of a constant twist along the specimen. The amount of tilt necessary to produce a twist which roughly nullified the effect of the other imperfections was determined by trial and error during preliminary elastic tests. By this device, the central angle of twist was usually kept below $\frac{1}{2}^\circ$, until in the neighbourhood of the critical moment a small increment of say 5 lb.in. in M_1 caused complete failure, the specimen assuming the buckled form shown in figure 44. The critical condition could therefore be determined quite

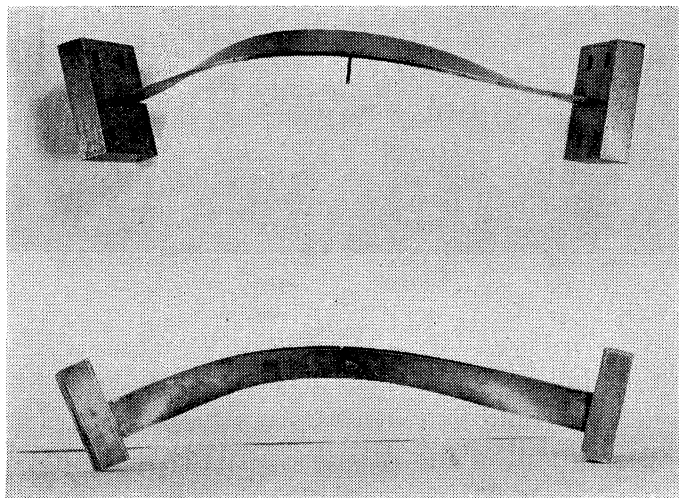


FIGURE 44

accurately. It was, of course, often a matter of hours before failure occurred, owing to the length of time required for plastic flow to take place after the addition of an increment of load, but the final collapse of the specimen always occurred very suddenly. Data concerning the rate of creep under constant load are not given here, as the results obtained were similar in character to the creep results described in part I.

Preliminary tests were carried out to measure the elastic secondary flexural rigidity and the torsional rigidity. The experimental arrangement adopted in these tests was similar to that already described in part II. One end of the specimen was bolted into an end fitting clamped so as to prevent rotation about each axis, and a light loading lever was bolted to the other free end of the specimen. A pure couple could be applied to the specimen about either the secondary principal axis or the longitudinal axis by means of loading wires attached to this lever, and the changes of curvature and twist were recorded in the usual way by means of small mirrors attached to small lengths of copper wire soldered to the specimen.

It was thought that the encastering blocks might not completely prevent twist at the ends of the specimen, and the elasticity of the end constraint against twist was accordingly measured during the torsion test, one of the mirrors being attached to the specimen 0.2 in. from the

encastering block and the end rotation deduced by interpolation. If the encastering torque corresponding to an end rotation θ is $\lambda\theta$, it may readily be shown that the critical buckling moment is reduced by a factor $(1-\eta)$, where

$$\eta = \frac{2C}{\lambda L(1-C/A)},$$

provided that η is small.

Five tests were carried out on the heat treated material. Tests 1 and 2 were on specimens cut from the stock A , and tests 3, 4 and 5 were on specimens cut from the stock B . The results of a single test 6, carried out on material cut from the stock A in the 'as received' condition, are also included. The dimensions of each specimen, the measured values of B_E , C and η , and the critical moment calculated on the assumption of elastic behaviour, are given in Table 14.

TABLE 14

specimen	mean depth (in.)	mean breadth (in.)	length (in.)	$B_E \times 10^{-3}$ (lb.in. ²)	$C \times 10^{-3}$ (lb.in. ²)	η (%)	elastic M_{cr} (lb.in.)
1	1.0008	0.1271	11.60	5.15	7.43	1.5	1684
2	1.0010	0.1271	12.69	5.16	7.42	0.4	1557
3	0.9995	0.1268	12.68	5.09	7.31	1.0	1529
4	0.9992	0.1266	17.75	5.07	7.28	2.0	1075
5	0.9994	0.1266	17.68	5.07	7.28	0	1102
6	1.0010	0.1269	11.90	5.10	7.55	0	1673

After a small correction due to the elasticity of the end fittings had been applied, the sum Δ_1 of the dial gauge readings could be taken as proportional to the primary curvature. In figures 45 to 50 the observations of the primary bending moment M_1 are shown plotted against Δ_1 , together with theoretical curves fitted to the observations in accordance with the theory given in part I. It will be seen that the observations deviate prematurely from the elastic line, owing to the effect of the initial imperfections in causing secondary bending and torsion stresses to develop.

From the theoretical curves the value of κ_1/κ_Y at any value of the curvature could be deduced, and the values of A/A_E and B/B_E calculated from the theory given in part I. The value of the critical lateral buckling moment at that value of the curvature could then be calculated. A curve relating this critical moment to the curvature could therefore be plotted on each diagram, and the intersection of this curve with the theoretical primary flexure curve then indicated the values of the primary bending moment and curvature at which buckling should occur. Such curves are shown in figures 45 to 50. The value of κ_1/κ_Y at which buckling should have occurred, together with the value of μ , the ratio of upper to lower yield stress, is also given.

The actual bending moment at which buckling occurred is marked on the prolongation of the theoretical primary flexure curves, together with the time which elapsed between the application of the last increment of load and failure.

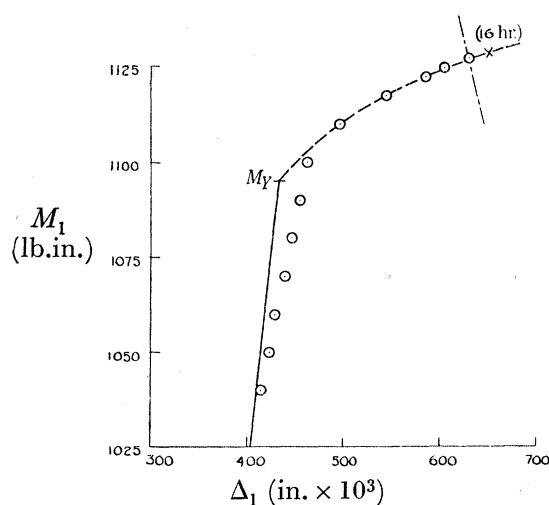
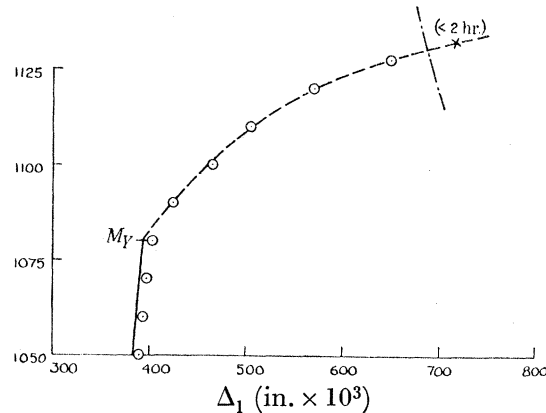
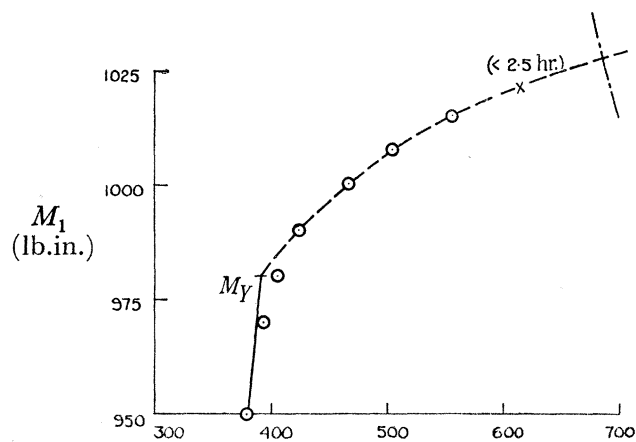
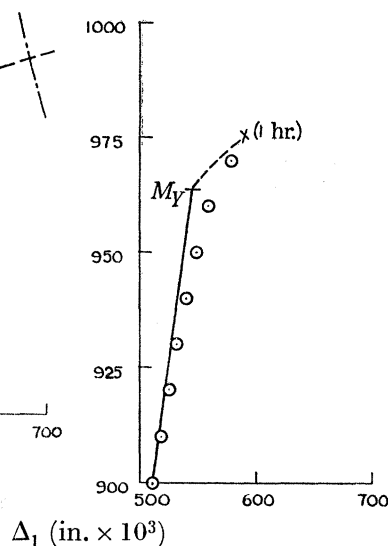
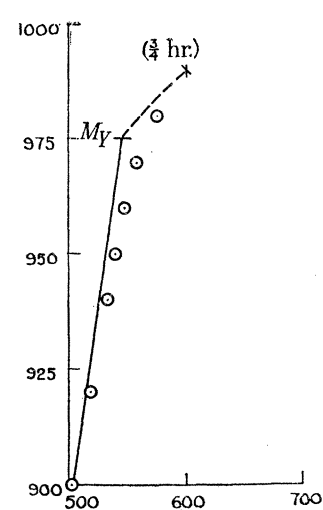
Data concerning the central angle of twist during each test are not reproduced here in detail, but the value of the central angle of twist before the application of the last increment of load is given in table 15, together with the corresponding value of the bending moment.

YIELDED MILD STEEL BEAMS

239

TABLE 15

test	1	2	3	4	5	6
M_1 (lb.in.)	1127	1128	1015	970	980	1401
twist (deg.)	0.02	0.43	0.69	0.63	0.39	3.04

FIGURE 45. Test 1. $\mu = 1.42$, $\kappa_1/\kappa_Y = 1.45$.FIGURE 46. Test 2. $\mu = 1.40$, $\kappa_1/\kappa_Y = 1.75$.FIGURE 47. Test 3. $\mu = 1.40$,
 $\kappa_1/\kappa_Y = 1.76$.FIGURE 48. Test 4. $\mu = 1.4$,
 $\kappa_1/\kappa_Y = 1$.FIGURE 49. Test 5.
 $\mu = 1.4$, $\kappa_1/\kappa_Y = 1$.

— elastic line; --- theoretical primary flexure curve; — · — theoretical buckling moment curve; ○ observations of Δ_1 ; × observed buckling moment.

It will be seen that in tests 1, 2 and 3 quite satisfactory agreement exists between the experimental and theoretical buckling moments, although in test 3 buckling occurred somewhat prematurely.

Tests 4 and 5 were carried out to verify the sudden failure at yield due to the finite drop in the secondary flexural rigidity. In test 4, for example, the critical moment if the specimen remained elastic would have been 1075 lb.in. On the assumption that the value of μ was 1.40 the value of B/B_E at yield would drop to 0.767, thereby reducing the critical moment

to 937 lb.in. The specimen failed at a primary bending moment of 975 lb.in., when it was evident that yield had occurred, although slight deviations from the elastic line due to the effect of the imperfections were detectable at somewhat lower moments. In test 5 the critical moment if the specimen remained elastic would have been 1102 lb.in., dropping to 961 lb.in. at yield. The specimen actually failed at 990 lb.in.

Test 6 was a preliminary test carried out on the material as received. Owing to cold working during the finishing process the upper yield point was probably destroyed near the

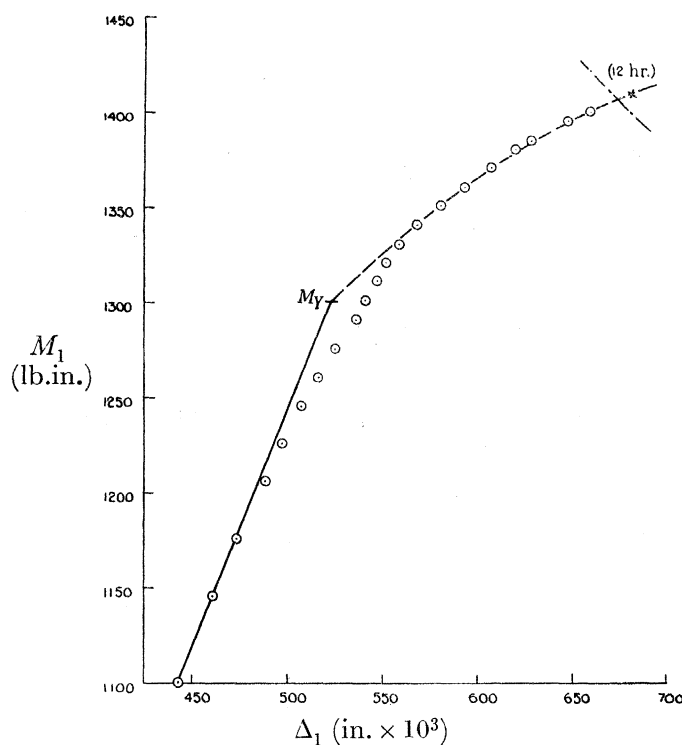


FIGURE 50. Test 6. $\mu = 1.24$, $\kappa_1/\kappa_Y = 1.29$.

— elastic line; --- theoretical primary flexure curve; —·— theoretical buckling moment curve; ⊙ observations of Δ_1 ; × observed buckling moment.

surface of the specimen, and residual stresses might also be expected to be present. Nevertheless, the observations of Δ_1 conformed surprisingly well to a theoretical relation assuming $\mu = 1.24$, particularly in view of the fact that this test was carried out without tilting one of the end fittings, so that the central angle of twist was larger than in the previous tests. There was close agreement between the theoretical and experimental buckling moments.

17. DISCUSSION

A theoretical discussion has been given which enables the critical load causing lateral buckling of a mild steel beam of rectangular cross-section to be predicted for those cases in which the beam has partially yielded. The theory takes no account of strain hardening, for it is assumed that indefinite extension or contraction of a longitudinal fibre can take place under a constant stress, the lower yield stress. However, in many cases lateral buckling would take place before extensions sufficiently large to cause strain hardening would occur.

The critical load which is calculated is the load at which the beam, if initially perfectly straight and free from twist, would deflect laterally out of the plane of flexure and simultaneously develop twist while the applied load was held constant. At this value of the load the lateral deflexion and twist, hitherto zero, become indeterminate. In a recent paper by Shanley (1947), it was pointed out that in cases of plastic buckling it may be possible to find a critical load, lower than the critical load defined in the conventional manner just given, above which deflexions may develop with increasing load. If the load exceeds this lower critical load, and an increment of load is applied, it is then possible for the beam to remain in equilibrium either by remaining straight or by deflecting by a definite amount which is determined by the magnitude of the load increment. However, large deflexions can only develop at the conventional critical load. In terms of the particular problem discussed in this paper, Shanley's concept is that secondary flexure occurs while the primary loading moment is increasing, so that the lateral deflexion and twist take place under increasing load.

If the primary bending moment is permitted to increase while secondary flexure is taking place, the unloading zones of figure 6 tend to disappear. This implies a reduction in the value of the secondary flexural rigidity, for in the previous case part of this rigidity was derived from the unloading zones. If the increment in the primary bending moment is sufficiently high, the unloading zones will disappear entirely, and the secondary flexural rigidity will then be as low as possible for the particular value of the primary bending moment under consideration. In fact this lowest value B' of the secondary flexural rigidity B will be the value for a beam of rectangular cross-section of depth $2pd$ which behaves elastically, so that $B' = \frac{4}{3} E p d b^3 = p B_E$. Thus in the case of pure bending, the lowest value M' of the applied bending moment at which lateral deflexion could occur with increasing load is given by finding the value of p which satisfies the equations

$$M' = \frac{\pi}{L} \sqrt{\left(\frac{B'C}{\left(1 - \frac{B'}{A}\right) \left(1 - \frac{C}{A}\right)} \right)} = M_Y \left[1 + (1 - p^2) \left(\frac{3}{2\mu} - 1 \right) \right].$$

While Shanley's concept of the bifurcation of equilibrium which arises in plastic buckling is of considerable theoretical interest, it is felt that in practice the conventional critical load should be considered as of greater importance, for it is this load at which actual collapse occurs. In practical testing, the possible growth of deflexion under increasing load in the manner described by Shanley would be masked by the inevitable deflexions arising owing to initial imperfections in the beam. Moreover, it is known that equilibrium is not reached after the application of a load increment until plastic flow has been allowed to proceed for several hours, so that the experimental reproduction of lateral deflexion and twist developing simultaneously with increase of load would be extremely difficult.

A final point which should be mentioned is that the results of the present paper cannot be immediately extended to cover cases of beams of Γ and other sections. A beam of Γ -section, for instance, derives some of its torsional stiffness from the differential bending of its flanges if the ends of the beam are prevented from warping (Timoshenko 1936). In this case a system of longitudinal stresses arises in the flanges which reduces approximately to bending moments of opposite sign in the flanges, tending to bend the flanges in their own plane. The variation of these bending moments along the length of the beam produces transverse shear forces in the planes of the flanges, which together constitute a couple offering additional

242 B. G. NEAL ON LATERAL INSTABILITY OF STEEL BEAMS

resistance to torsion. The analysis given in this paper would require some modification to take this effect into account, but it has been shown that such an effect only alters the critical buckling load of beams of rectangular cross-section by a negligible amount (Timoshenko 1921).

REFERENCES

- Baker, J. F. 1949 *J. Inst. Civ. Engrs*, **31**, 188.
 Baker, J. F. & Roderick, J. W. 1940 *Trans. Inst. Weld.* **3**, 83.
 Cook, G. 1931 *Phil. Trans. A*, **230**, 103.
 Federhofer, K. 1931 *S.B. Akad. Wiss. Wien*, **140**, 237.
 Fisher, R. A. 1941 *Statistical methods*. 8th ed. Edinburgh: Oliver & Boyd.
 Fox, L. 1947 *Proc. Roy. Soc. A*, **190**, 31.
 Hill, R., Lee, E. H. & Tupper, S. J. 1947 *Proc. Roy. Soc. A*, **191**, 278.
 Howard, J. V. & Smith, S. L. 1925 *Proc. Roy. Soc. A*, **107**, 113.
 Jevons, J. D. 1925 *J. Iron Steel Inst.* **111**, 191.
 Jevons, J. D. 1927 *Engineering*, **123**, 155.
 Love, A. E. H. 1920 *Elasticity*. 3rd ed., p. 72. Cambridge University Press.
 Morrison, J. L. M. 1939 *Proc. Instn Mech. Engrs*, **142**, 193.
 Muir, J. & Binnie, D. 1926 *Engineering*, **122**, 743.
 Nadai, A. 1931 *Plasticity*. 1st ed., p. 75. New York: McGraw Hill.
 Nakanishi, F. 1929 *Proc. World Engng Congr., Tokio*, **3**, 235.
 Prandtl, L. 1924 *Proc. 1st Int. Congr. Appl. Mech., Delft*, p. 43.
 Reissner, H. 1904 *S.B. berl. math. Ges.* **3**, 53.
 Reuss, A. 1930 *Z. angew. Math. Mech.* **10**, 266.
 Robertson, A. & Cook, G. 1913 *Proc. Roy. Soc. A*, **88**, 462.
 Shanley, F. R. 1947 *J. Aero. Sci.* **14**, 261.
 Shepherd, W. M. 1948 *J. Instn Mech. Engrs*, **159**, 95.
 Smith, C. A. M. 1909 *Proc. Instn. Mech. Engrs*, **77**, 1237.
 Tables 1942 *Interpolation and allied tables*. H.M. Stationery Office.
 Timoshenko, S. 1921 *Proc. Lond. Math. Soc.* **20**, 389.
 Timoshenko, S. 1936 *Elastic stability*. 1st ed., p. 239. New York: McGraw Hill.

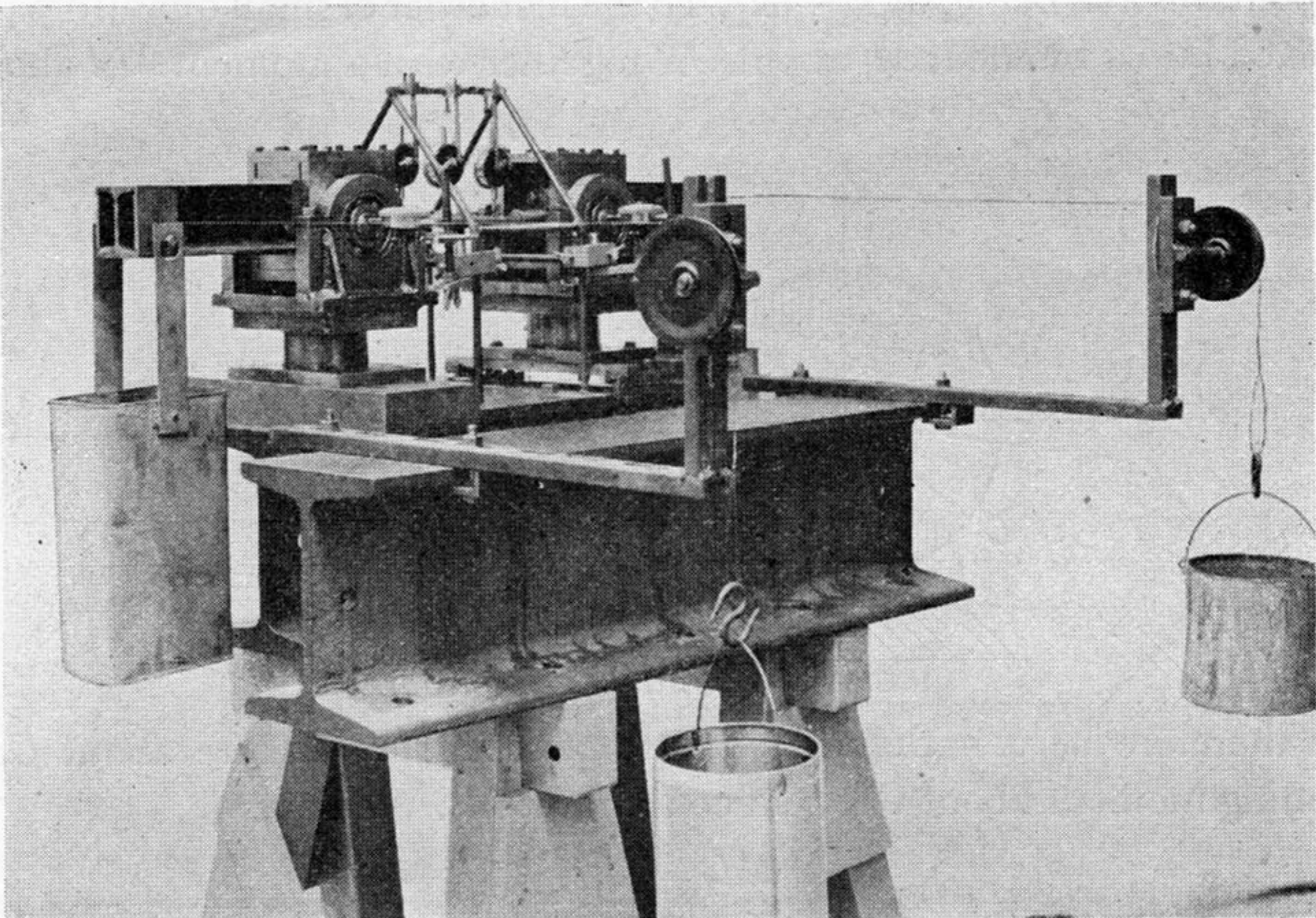


FIGURE 15

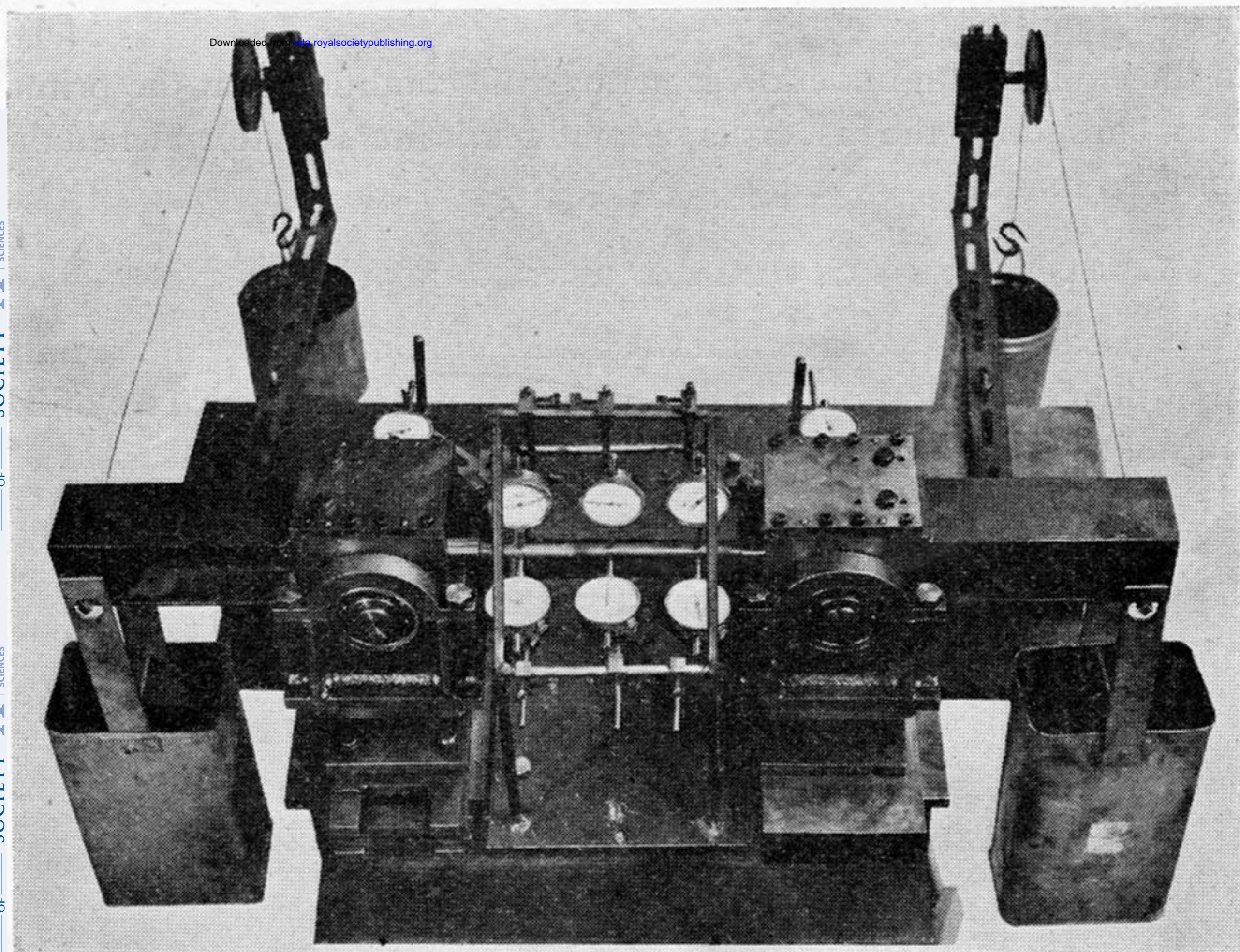


FIGURE 16

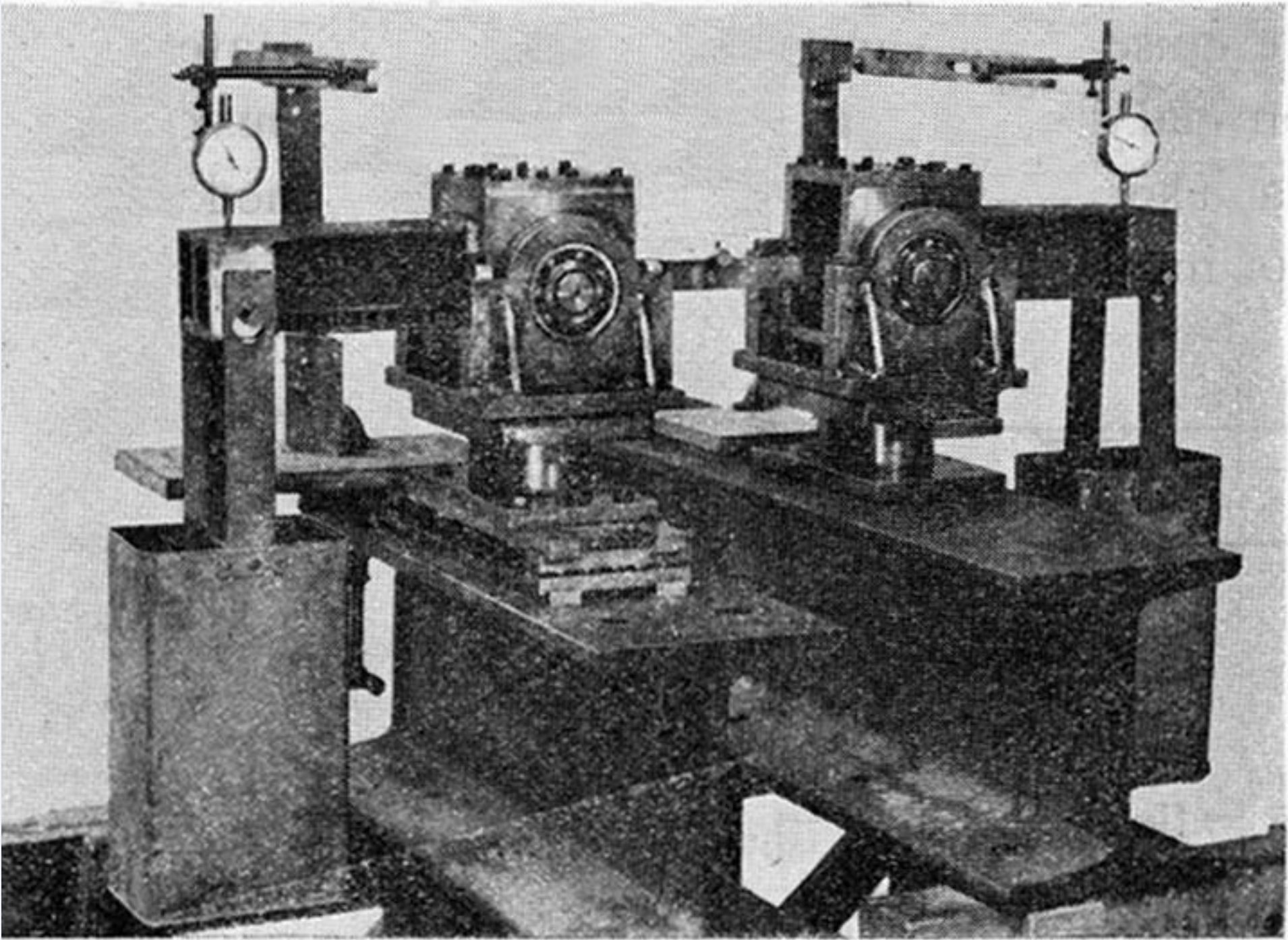


FIGURE 43

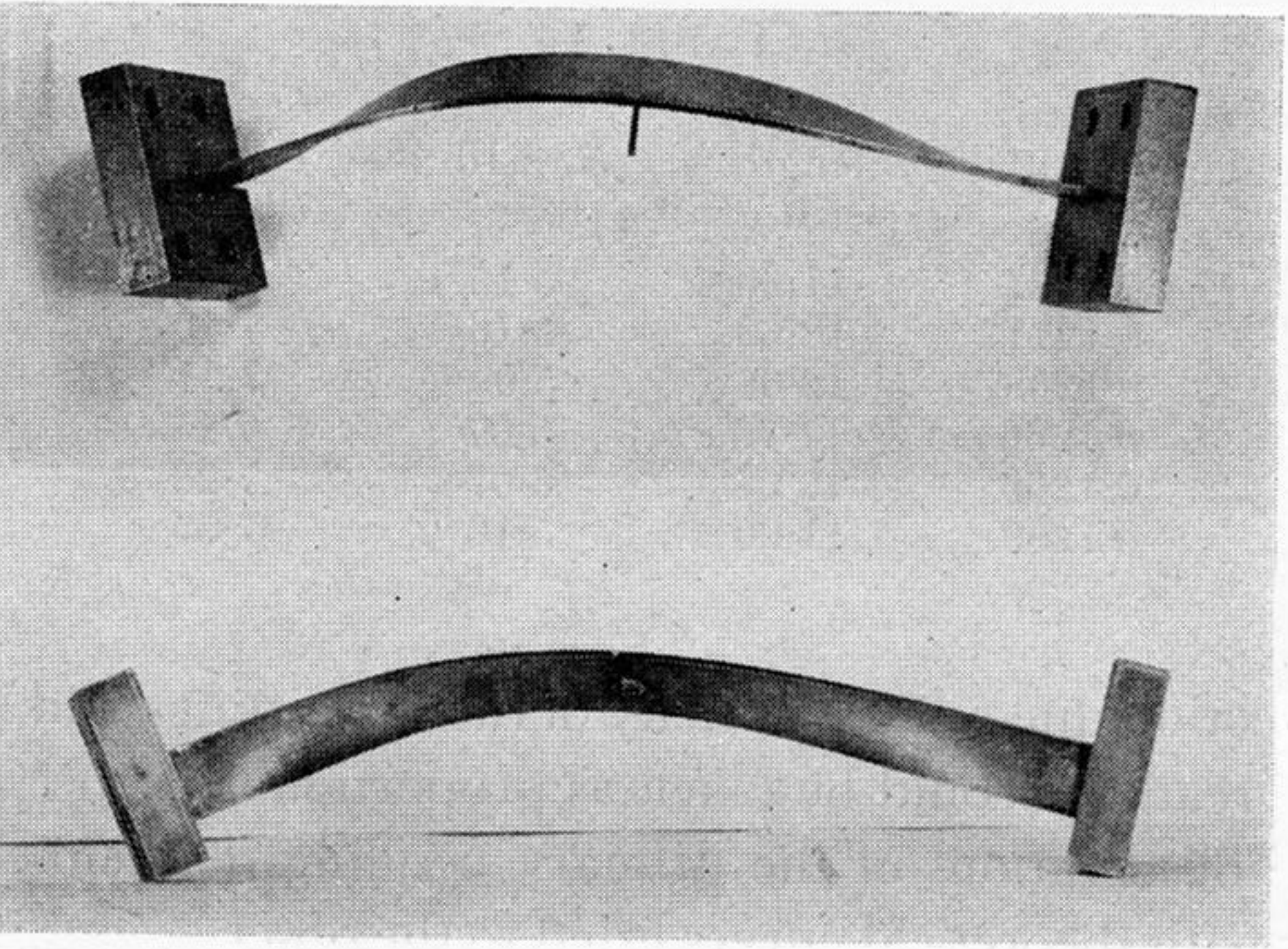


FIGURE 44